Synthesis and Preliminary Characterization of Some Polyester Rotaxanes

Harry W. Gibson,* Shu Liu, Pierre Lecavalier, Charles Wu, and Ya Xi Shen

Contribution from the Department of Chemistry, Virginia Polytechnic Institute and State University, Blacksburg, Virginia 24061

Received September 1, 1994[⊗]

Abstract: A series of polyester rotaxanes containing polysebacate backbones [decamethylene, tri(ethyleneoxy), and 1,4-butylene] and ethylene oxide-based crown ethers [30-crown-10, 42-crown-14, 60-crown-20, and bis(*p*-phenylene)-34-crown-10] was synthesized via step growth polymerizations using diacid chloride−diol and transesterification reactions. The polyrotaxanes were purified by multiple reprecipitations in good solvents for the crown ethers, and the physical linkage of the crown ether to the polymeric backbone was confirmed by a variety of experiments, including hydrolysis, NMR, GPC, and VPO. Up to 55 wt % macrocycle was incorporated, depending on the size and shape of the macrocycle and the feed ratios employed. In all cases, the solubilities of the polyrotaxanes were strongly influenced by the cyclic component; enhanced solubilities in polar solvents were observed relative to the simple parent polysebacates. Mark−Houwink K and a values were also strongly affected by rotaxane formation; in the case most thoroughly investigated, K decreased by almost 2 orders of magnitude and a doubled. Interpretation of this observation is complicated by the changes in solubility. Thermal behavior was also affected. In the tri(ethyleneoxy) system, T_g is lowered in the rotaxanes; in the 60-crown-20 system, the macrocycle crystallized! The poly(butylene sebacate) 60-crown-20 and 42-crown-14 systems also possessed two crystalline phases, a crown ether phase and a poly(butylene sebacate) phase. These exciting result demonstrate the mobility of the macrocycle along the polyester backbone in melt and solution states, allowing aggregation and crystallization without dethreading.

Introduction

I. Molecular Architectures. Chemists' fascination with molecular architectures has allowed the development and testing of theoretical concepts and provided entirely new and largely unforseen areas of applications. Developments in host−guest chemistry[1] and the utilization of such concepts in supramolecular chemistry,[2] both Nobel prize-winning activities, provide inspiring proof that this is a challenging but fruitful endeavor.

Organic chemistry abounds with molecules whose shapes mimic familiar macroscopic objects, giving rise to names such as housane, cubane, felicene, lepidopterene, and footballane.[3] The shapes of molecules are a reflection of their *topography*. A related property is *topology*, which is concerned with the connectivity of the atoms in the molecule.[4] Isomerism associated with molecules with the same topology is called *topological isomerism*; examples of this are provided by cyclic species and their knotted analogs.

Polymer chemists have utilized their synthetic skills to produce linear, branched, or cyclic architectures. These architectures represent different topologies; the number of ends varies because of different connectivities. The recently developed dendritic class[5] represents an extreme in this sense; in the divergent approach, the number of ends increases exponentially with every generation of monomer addition. Cyclic polymers have no ends; therefore, they lie at the other end of the topological spectrum.[6] Graft copolymers have topologies different from those of statistical and block systems. All of these architectural modifications produce changes in physical properties. That is, the properties of a polymer depend not only on its chemical constitution and molecular weight but also in a very sensitive way on its architecture.

II. Rotaxanes. Rotaxanes are compounds comprised of cyclic molecules penetrated by linear molecules, without a covalent bond between the components. The first rotaxanes were reported in 1967.[7] Since that time, many examples of low molecular weight rotaxanes of varying complexity have been reported (*inter alia* refs 8−10).

The key step in the construction of a rotaxane is the creation of a condition which allows the threading of the linear chain through the cyclic component to take place. In principle, threading can be achieved through two approaches. Equation 1 shows the threading equilibrium for a monorotaxane and its topological isomers, the cyclic and linear components. When a strongly attractive interaction is present between the cyclic and the linear components, ΔH is the determining factor in eq 1, and K may be large, i.e., greater than 10 L/mol. Such threading is referred to as directed (or template) threading. Alternatively, in the absence of strong attractive interactions between the cyclic and the linear components, i.e., ΔH is only

[⊗] Abstract published in *Advance ACS Abstracts,* January 1, 1995.

(1) Cram, D. J. *Angew. Chem., Int. Ed. Engl.* **1988**, *27*, 1009.

(2) Lehn, J.-M. *Angew. Chem., Int. Ed. Engl.* **1988**, *27*, 89.

(3) For an entertaining, light-hearted discussion of this area, see: Nickon, A.; Silversmith, E. F. *Organic Chemistry, the Name Game*; Pergammon Press: New York, 1987.

(4) Walba, D. *Tetrahedron* **1985**, *41*, 3161.

(5) Tomalia, D. A.; Durst, H. D. *Top. Curr. Chem.* **1993**, *165*, 193. Newkome, G. R.; Moorefield, C. N.; Baker, G. R.; Behera, R. K.; Escamillia, G. H.; Saunders, M. J. *Angew. Chem., Int. Ed. Engl.* **1992**, *31*, 917. Gitsov, I.; Fréchet, J. M. J. *J. Chem. Soc.* **1993**, *26*, 6536. Xu, Z.; Moore, J. S. *Angew. Chem., Int. Ed. Engl.* **1993**, *32*, 1354. de Brabender-van den Berg, E. M. M.; Meijer, E. W. *Angew. Chem., Int. Ed. Engl.* **1993**, *32*, 1308. Mekelburger, H. B.; Jaworek, W.; Vögtle, F. *Angew. Chem., Int. Ed. Engl.* **1992**, *31*, 1571 and references therein.

(6) Semlyen, A. *Cyclic Polymers*; Elsevier Applied Science Publishers: New York, 1986.

(7) Schill, G.; Zollenkopf, H. *Nachr. Chem. Tech.* **1967**, *79*, 149; *Ann. Chem.* **1969**, *721*, 53. Harrison, I. T.; Harrison, S. *J. Am. Chem. Soc.* **1967**, *89*, 5723.

(8) Harrison, I. T. *J. Chem. Soc., Chem. Commun.* **1972**, 231; *J. Chem. Soc., Perkin Trans. 1* **1974**, 301; *J. Chem. Soc., Chem. Commun.* **1977**, 384.

(9) Agam, G.; Gravier, D.; Zilkha, A. *J. Am. Chem. Soc.* **1976**, *98*, 5206. Agam, G.; Zilkha, A. *J. Am. Chem. Soc.* **1976**, *98*, 5214.

(10) Schill, G. *Catenanes, Rotaxanes and Knots*; Academic Press: New York, 1971. Schill, G.; Logemann, E.; Littke, W. *Chem. Unserer Zeit* **1984**, *18*, 129. Schill, G.; Beckmann, W.; Schweikert, N.; Fritz, H. *Chem. Ber.* **1986**, *119*, 2647.

0002-7863/95/1517-0852$09.00/0

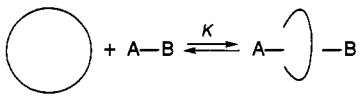

(1)

$$\ln K = -\Delta G/RT = -(\Delta H - T\Delta S)/RT$$

slightly negative, zero, or perhaps slightly positive, $T\Delta S$ becomes the determining factor in eq 1. This kind of threading is referred to as statistical threading, and K is on the order of 0.01−10 L/mol. The directed approach offers better control of the threading process; however, as described below, since this approach requires that both the cyclic and the linear components possess special functionalities and complementary geometries, often an additional step is needed to remove the attractive interaction between the two components after the threading. Statistical threading is more attractive in general because it can be applied to any linear system. In practice, the threading efficiency of this process can be improved by application of Le Chatelier's principle through use of a large excess of one of the components, either the cyclic or the linear species.

The early examples of rotaxanes were made by statistical threading, producing what we refer to as *homorotaxanes*, in which the chemical structures of the cyclic and linear species are identical or nearly so, e.g., hydrocarbon linear and hydrocarbon cyclic, as opposed to *heterorotaxanes*, in which the linear and cyclic entities are chemically distinct, e.g., hydrocarbon linear and polyether cyclic. The threading in homorotaxanes is driven only by the entropic term and is therefore temperature independent.[9] As in any equilibrium, the ratio of cyclic and linear components is important, as are their absolute concentrations. Geometric factors of importance are the size and rigidity of the two components.

Experiments by Schill et al.[10] and Harrison[8] led to the conclusion that the cyclic compound must contain at least 22 carbon atoms, or presumably a total of at least 22 carbon, oxygen, and nitrogen atoms, in order to be penetrated by a methylene chain, whose cross sectional diameter is approximately 4.5 Å. By similar experiments, it was established that triphenylmethyl (trityl) end-blocking groups could constrain rings up to and including 28- or 29-membered. The larger tris-(*p-tert*-butylphenyl)methyl end-blocking group was shown to be capable of retaining rings up to and including 42-membered.

Agam and co-workers concluded that for flexible systems ring size is the most important geometric variable in determining the efficiency of threading.[9] Agam et al. suggested that threadings of a large ring by several linear molecules are possible, as are penetrations of several rings by a single long linear species.

Sauvage and co-workers have utilized the template effect. Specifically, by reaction with Cu^+, a tetrahedral complex, a stable rotaxane, is formed (around the metal template) by threading of a cyclic phenanthroline compound with a claw-shaped phenanthroline bisphenol. Sauvage et al. formed catenanes and knots by cyclization of the resultant bisphenol rotaxane complexes.[11] We prepared a monomeric rotaxane by end-capping the tetrahedral copper complex and then removing the Cu^+ ion.[12]

Charge transfer interactions between the two components can also provide an enthalpic attractive interaction that helps to drive the threading equilibrium (eq 1) to the right, in concert with hydrogen bonding and dipole−dipole interactions. This is the approach reported by Stoddart and co-workers, who formed a stable complex from paraquat and bis(*p*-phenylene)-34-crown-10 (BPP) and found by X-ray crystallography that the acceptor, paraquat, resided within the cavity of BPP, the donor;[13a] the cavity of BPP is open in its low-energy conformations[13b] and in fact is essentially unchanged by complexation. Stoddart and co-workers have reported intriguing extensions of these concepts.[13c]

Recently, other template-directed syntheses have been studied. Ogino synthesized and studied some properties of rotaxanes consisting of cyclodextrins threaded by α,ω-diaminoalkanes coordinated to cobalt(III) complexes.[14] Lawrence et al. reported the self-assembly of a threaded molecular loop in 71% yield from a diammonium chloride salt and heptakis(2,6-*O*-methyl)-β-cyclodextrin in aqueous solution.[15] Rotaxanes based upon cyclodextrins and oligo(ethylene glycol)s have been reported recently by Harada et al.[16] The workers were able to link the macrocycles together to form a tube and then release the linear component.

III. Polymeric Rotaxanes. Polymeric rotaxanes or "polyrotaxanes" are comprised of macrocycles threaded by linear polymer molecules, with no chemical bonding between the cyclic and the linear components (Figure 1). Polyrotaxanes afford enhanced capability for property modification. They may be viewed as physical analogs of traditional copolymers. However, due to the potential for the cyclic component to move laterally along the linear backbone as well as circumferentially, these systems are expected to possess properties distinct from those of traditional covalently bonded copolymers or analogous blends. Potential areas of utilization include improved interfacial bonding (adhesion, blend compatibilization) and processability (enhanced solubility) and improved control of thermal properties (glass transition, melting), viscosity, and molecular ordering.

Ogata and co-workers claimed synthesis of the first polyrotaxanes by reaction of β-cyclodextrin and inclusion complexes of diamines with diacid chlorides to yield main chain poly(amide/rotaxane)s.[17]

Maciejewski reported the production of a main chain polyrotaxane by radiation-induced polymerization of the crystalline adduct of vinylidene chloride and β-cyclodextrin (β-CD) or by

(11) Dietrich-Buchecker, C. O.; Sauvage, J.-P. *Chem. Rev.* **1987**, *87*, 795. Sauvage, J.-P. *Acc. Chem. Res.* **1990**, *23*, 319. Chambron, J. C.; Dietrich-Buchecker, C.; Sauvage, J.-P. *Top. Curr. Chem.* **1993**, *165*, 131. Chambron, J. C.; Harriman, A.; Heitz, V.; Sauvage, J.-P. *J. Am. Chem. Soc.* **1993**, *115*, 7419. Nierengarten, J.-F.; Dietrich-Buchecker, C. D.; Sauvage, J.-P. *J. Am. Chem. Soc.* **1994**, *116*, 375. Armaroli, N.; Balzani, V.; De Cola, L.; Hemmert, C.; Sauvage, J.-P. *New J. Chem.* **1994**, *18*, 775. Livoreil, H.; Dietrich-Buchecker, C. O.; Sauvage, J. P. *J. Am. Chem. Soc.* **1994**, *116*, 9399.

(12) Wu, C.; Lecavalier, P. R.; Shen, Y. X.; Gibson, H. W. *Mater. Chem.* **1991**, *3*, 569.

(13) (a) Allwood, B. L.; Spencer, N.; Shahriari-Zavareh, H.; Stoddart, J. F.; Williams, D. J. *J. Chem. Soc., Chem. Commun.* **1987**, 1061; 1064. Stoddart, J. F. *Pure Appl. Chem.* **1988**, 467. (b) Slawin, A. M. Z.; Spencer, N.; Stoddart, J. F.; Williams, D. J. *J. Chem. Soc., Chem. Commun.* **1987**, 1070. (c) Stoddart, J. F. *Chem. Br.* **1991**, 714; *SynLett* **1991**, 445. Anelli, P.; Ashton, P. R.; Ballardini, R.; Balzani, V.; Delgado, M.; Gandolfi, M. T.; Goodnow, T. M.; Kaifer, A. E.; Philp, D.; Pietraskiewicz, M.; Prodi, L.; Reddington, M. V.; Slavin, A. M. Z.; Spencer, N.; Stoddart, J. F.; Vicent, C.; Williams, D. J. *J. Am. Chem. Soc.* **1992**, *114*, 193. Ashton, P. R.; Philp, D.; Spencer, N.; Stoddart, J. F.; Williams, D. J. *J. Chem. Soc., Chem. Commun.* **1994**, 181. Ambalino, D. B.; Ashton, P. R.; Reder, A. S.; Spencer, N.; Stoddart, J. F. *Angew. Chem., Int. Ed. Engl.* **1994**, *33*, 1286. Seiler, M.; Willner, I.; Joselevich, E.; Doron, A.; Stoddart, J. F. *J. Am. Chem. Soc.* **1994**, *116*, 3399.

(14) Ogino, H. *J. Am. Chem. Soc.* **1981**, *103*, 1303.

(15) Venkata, T.; Rao, S.; Lawrence, D. S. *J. Am. Chem. Soc.* **1990**, *112*, 3614.

(16) Harada, A.; Li, J.; Kamachi, M. *Nature* **1992**, *356*, 325; **1993**, *364*, 316; *Macromolecules* **1994**, *27*, 4538.

(17) Ogata, N.; Sanui, K.; Wada, J. *J. Polym. Sci., Polym. Lett. Ed.* **1975**, *14*, 459.

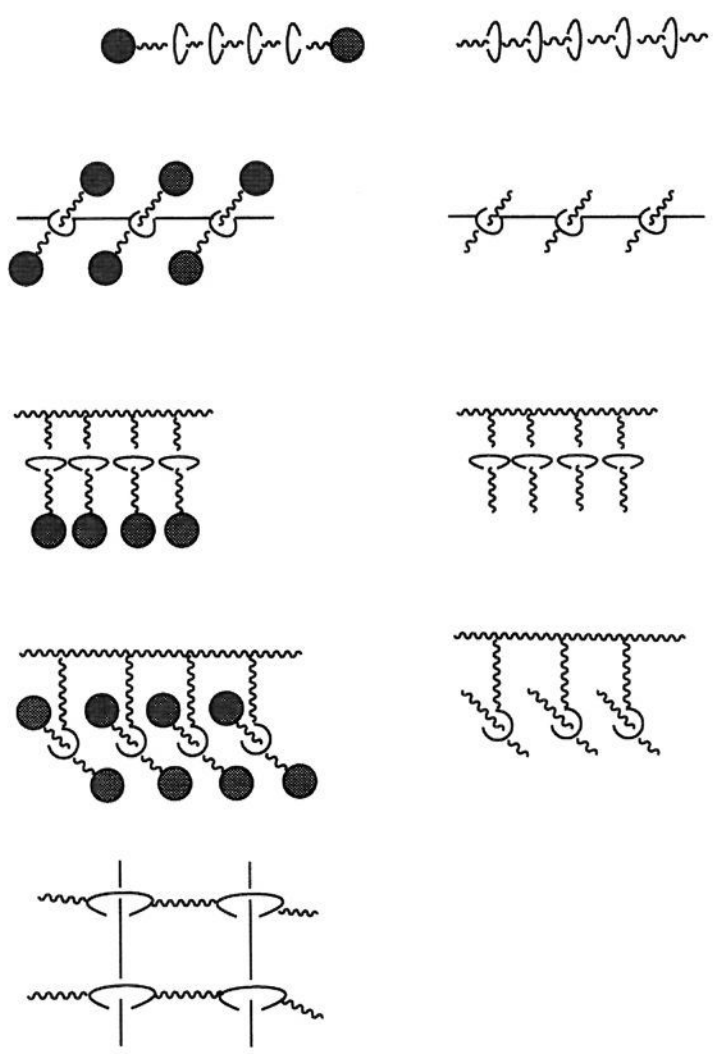

Figure 1. Schematic representations of various types of polymeric rotaxanes, i.e., polyrotaxanes. The straight and wavy lines represent linear species, the open circles or ellipses are cyclic components, and the closed circles represent bulky "blocking groups" which prevent diffusional dethreading of the cyclic species.

thermal polymerization of the components in dimethylformamide.[18] The polymer was 80% cyclodextrin by mass. The crystal structure was essentially the same as that of cyclodextrin.

Lipatova et al. carried out thermal polymerization of styrene in the presence of swollen (insoluble) cyclic urethanes [derived from di- and tri(ethylene glycol)s] and $ZnCl_2$ to produce crystalline main chain polyrotaxanes whose X-ray diffraction patterns matched those of the cyclic urethanes.[19] The number of rings incorporated varied from 0.05 to 0.14 per styryl unit.

A comblike, side chain polyrotaxane containing rotaxane units in the side chains has been synthesized by Born and Ritter[20] via the self-assembly process of 2,6-dimethyl-β-CD and the monofunctional blocking group *N*-(*p*-(triphenylmethyl)phenyl)-butanamide; the amino-functionalized rotaxane then was reacted with a polymer having anhydride sites along the chain.

Other workers have also utilized cyclodextrins as the cyclic components of polyrotaxanes. Wenz and Keller threaded preformed protonated polyamines through α-cyclodextrin and the di(*O*-methyl) derivative of β-CD.[21]

The threading of cyclic oligo(dimethylsiloxane)s by linear poly(dimethylsiloxane)s has been studied extensively by Semlyen, Mark, Frisch, Clarson, and co-workers.[22] The homorotaxane systems were analyzed by cross-linking the linear polymer and determining the percentage of threaded rings by exhaustive extraction of untrapped rings. A wide range of ring sizes was studied.

IV. Perspectives and Goals of the Present Work. It is the objective of our research program[12,23−31] to explore and exploit the novel topographic and topological features of polymeric rotaxanes by synthesis of a variety of polyrotaxanes in sufficient quantity to carry out traditional polymer characterization experiments on the solution and bulk states. These properties will be compared to those of the corresponding model linear polymers.

There are, in principle, four methods that could be applied to the synthesis of main chain polyrotaxanes: (1) threading of preformed cyclic molecules by preformed linear polymers; (2) formation of cyclic molecules in the presence of preformed linear polymers; (3) polymerization of stable rotaxane monomers; and (4) formation of linear polymers in the presence of preformed cyclic species. The results of Agam et al. show that the degree of threading of oligomeric linear species first increases and then decreases with increasing molecular weight,[9] presumably reflecting diminution of chain end concentration, although the effect of equilibration time should probably be re-examined. At higher molecular weights in neat systems, decreased mobility of chain ends as a result of high viscosity will also lower the threading rate and perhaps the efficiency. Thus, as will be shown below method 1 is generally not an efficient way to make polyrotaxanes.

Cyclization reactions usually require dilute conditions. In order to form polyrotaxanes by cyclization in the absence of a template effect, the polymer would have to serve as the solvent in method 2. While this might be tenable for some cases, method 2 does not appear to be a generally useful synthetic method for polyrotaxanes.

Inspired by the results of Stoddart et al., we have utilized complexation to prepare a series of difunctional rotaxane monomers containing BPP (**4** below) and difunctional quaternary

(18) Maciejewski, M. *J. Macromol. Sci. Chem.* **1979**, *A18* (1), 77. Maciejewski, M.; Gwizdowski, A.; Peczakand, P.; Pietrak, A. *J. Macromol. Sci. Chem.* **1979**, *A13* (1), 87.

(19) Lipatov, Y. S.; Lipatova, T. E.; Kosyanchuk, L. F. *Adv. Polym. Sci.* **1989**, *88*, 49. Lipatova, T. E.; Kosyanchuk, L. F.; Gomza, Y. P.; Shilov, V. V.; Lipatov, Y. S. *Dokl. Akad. Nauk SSSR, Engl. Transl.* **1982**, *263*, 140. Lipatova, T. W.; Kosyanchuk, L. F.; Shilov, V. V.; Gomza, Y. P. *Polym. Sci., U.S.S.R., Engl. Transl.* **1985**, *27*, 622.

(20) Born, M.; Ritter, H. *Makromol. Chem., Rapid Commun.* **1991**, *12*, 471. Born, M.; Koch, T.; Ritter, H. *Acta Polym.* **1994**, *45*, 68.

(21) Wenz, G.; Keller, B. *Angew. Chem., Int. Ed. Engl.* **1992**, *31*, 197. Wenz, G.; Wolf, F.; Wagner, M.; Kubik, S. *New J. Chem.* **1993**, *17*, 729. Wenz, G. *Angew. Chem., Int. Ed. Engl.* **1994**, *33*, 803.

(22) Garrido, L.; Mark, J. E.; Clarson, S. J.; Semlyen, J. A. *Polym. Commun.* **1985**, *26*, 53. Garrido, L.; Mark, J. E.; Clarson, S. J.; Semlyen, J. A. *Polym. Commun.* **1985**, *26*, 55. Clarson, S. J.; Mark, J. E.; Semlyen, J. A. *Polym. Commun.* **1987**, *27*, 244. Fyvie, T. J.; Frisch, H. L.; Semlyen, J. A.; Clarson, S. J.; Mark, J. E. *J. Polym. Sci., Poly. Chem.* **1987**, *A25*, 2503. DeBolt, L. C.; Mark, J. E. *Macromolecules* **1987**, *20*, 2369. Mark, J. E. *New. J. Chem.* **1993**, *17*, 703. Clarson, S. J. *New J. Chem.* **1993**, *17*, 711. Joyce, S. J.; Hubbard, R. E.; Semlyen, J. A. *Eur. Polym. J.* **1993**, *29*, 305.

(23) Shen, Y. X.; Engen, P. T.; Berg, M. A. G.; Merola, J. S.; Gibson, H. W. *Macromolecules* **1992**, *25*, 2786. Loveday, D.; Wilkes, G. L.; Shen, Y. X.; Bheda, M.; Gibson, H. W. *J. Macromol. Sci. Chem.*, in press.

(24) Shen, Y. X.; Gibson, H. W. *Macromolecules* **1992**, *25*, 2058. Shen, Y. X.; Xie, D.; Gibson, H. W. *J. Am. Chem. Soc.* **1994**, *116*, 537.

(25) Gibson, H. W.; Engen, P. T. *New J. Chem.* **1993**, *17*, 723.

(26) Gibson, H. W.; Bheda, M. C.; Engen, P. T. *Prog. Polym. Sci.* **1994**, *19*, 843. Gibson, H. W.; Marand, H. *Adv. Mater.* **1993**, *5*, 11. Gibson, H. W.; Engen, P. T.; Shen, Y. X.; Sze, J.; Lim, C.; Bheda, M.; Wu, C. *Makromol. Chem., Macromol. Symp. Vol.* **1992**, *54/55*, 519.

(27) Preliminary account of the present work: Wu, C.; Bheda, M. C.; Lim, C.; Shen, Y. X.; Sze, J.; Gibson, H. W. *Polym. Commun.* **1991**, *32*, 204.

(28) Gibson, H. W.; Bheda, M. C.; Engen, P.; Shen, Y. X.; Liu, S.; Zhang, H.; Gibson, M. D.; Delaviz, Y.; Lee, S. H.; Wang, L.; Rancourt, J.; Taylor, L. T. *J. Org. Chem.* **1994**, *59*, 2186.

(29) Bheda, M.; Merola, J. S.; Woodward, W. A.; Vasudevan, V.; Gibson, H. W. *J. Org. Chem.* **1994**, *59*, 1694.

(30) We have adopted this system of nomenclature based on the fact that polyrotaxanes are physical analogs of copolymers. Thus, in accordance with the IUPAC system, in which the name contains the designations of the two components separated by the abbreviation for random, block, or graft type of architecture, we use the abbreviation "rotaxa" to designate the rotaxane architecture.

(31) Lecavalier, P. R. Engen, P. T.; Shen, Y. X.; Joardar, S.; Ward, T. C.; Gibson, H. W. *Am. Chem. Soc. Div. Polym. Chem. Polym. Prepr.* **1989**, *30* (1), 189.

Scheme 1

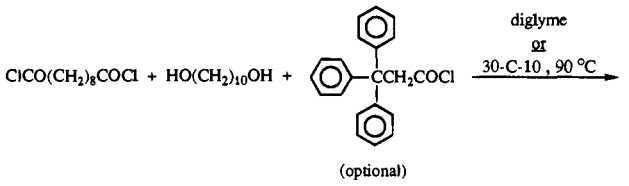

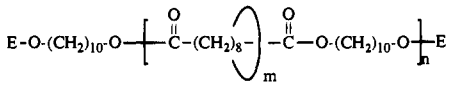

5a: m/n = 0, E = H, Model Polymer

5b: m/n = 0, E = $COCH_2C(C_6H_5)_3$, End Blocked Model Polymer

6: m/n > 0, E = $COCH_2C(C_6H_5)_3$, Polyrotaxane ⬯ = 30-crown-10 (1)

salts of 4,4-bipyridine.[23] These can be formed essentially quantitatively *in situ* and used in polymerizations, as we have shown by synthesis of a series of elastomeric viologen-based segmented polyurethanes.[23] This represents one example of the use of method 3.

Polyrotaxanes can be prepared by the statistical method (method 4) by a variety of step and chain growth techniques. For example, we have reported syntheses of a family of polyurethane rotaxanes by threading crown ethers with tetra(ethylene glycol) and then polymerization with bis(*p*-isocyanophenyl)methane.[24] Free radical polymerization can also be used, as exemplified by synthesis of polyacrylonitrile rotaxanes from 60-crown-20.[25] Summaries of these syntheses and the unique physical properties of the resulting polyrotaxanes have also appeared, along with a complete review of low molecular weight systems.[26]

In this paper we will discuss the synthesis of a family of polyester rotaxanes[27] using step growth polymerization and the statistical threading of preformed macrocycles (method 4) and the isolation, characterization, and preliminary physical analyses of these novel polymeric materials.

Results and Discussion

Our plan for the synthesis was to carry out the polymerizations in the presence of a large amount of the macrocycle, in fact using crown ethers as solvents, so that maximal threading could take place in monomer, oligomer, and polymer stages, and the system was under the threading equilibrium condition throughout the polymerization. This constitutes method 4 noted above. Bulky groups were introduced to cap the polymer chain ends in some experiments, so that the threaded macrocycle would be physically locked and retained on the polymer backbone. The resultant polyrotaxane could then be purified without losing the threaded macrocycles.

We have chosen to focus initially on crown ethers as the macrocyclic components. The crown ethers **1**–**4** are the macrocycles employed in this work. We have previously reported syntheses of crown ethers **1**–**3** and others[28] and the crystal structures of **1** and its tetrahydrate.[29]

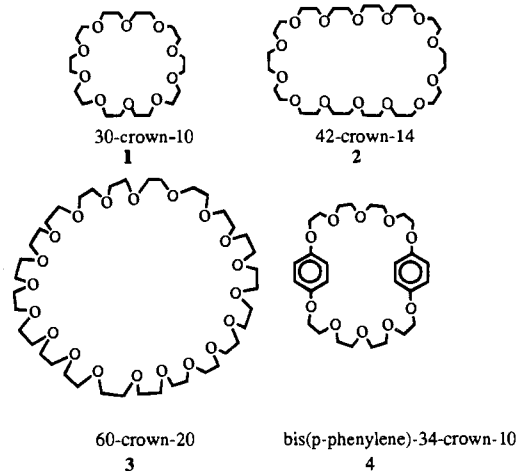

I. Diacid Chloride/Diol Polymerizations: Poly[(1,10-decamethylene sebacate)-rotaxa-(30-crown-10)] (6).[30] A. Model Studies. In model reactions (Scheme 1), sebacoyl chloride was reacted with a slight excess (≤1%) of 1,10-decanediol (Table 1, samples 157, 205, and 239) in diglyme; diglyme was chosen

Table 1. Poly(decamethylene sebacate) (**5**) and Poly[(decamethylene sebacate)-rotaxa-(30-crown-10)] (**6**) via Scheme 1

sample no.	polymer	diacid chloride/diol[a]	BG/diol[a]	30C10/diol[a]	*m*/*n*[b]	$10^{-3}\bar{M}_n$ NMR	$10^{-3}\bar{M}_n$ UV[d]	$10^{-3}\bar{M}_n$ GPC[e]	$10^{-3}\bar{M}_w$ GPC[e]	log K^t	a^f	$[\eta]^f$
157	**5a**[g]	0.989	0	0	0			7.7	13.0	−2.76	0.544	0.297
205	**5a**[h]	0.989	0	0	0			7.0	14.9	−3.08	0.643	0.383
239	**5a**[i]	0.996	0	0	0			8.3	27.5	−2.58	0.539	0.575
161	**5b**[g]	0.992	0.211[j]	0	0	13[c] 12[n]	10.7	7.7	11.8	−3.70	0.793	0.348
187	**5b**[k]	0.989	0.211[j]	0	0	30[c]	26.8	7.0	12.2	−3.24	0.670	0.296
203	**5b**[k]	0.989	0.211[j]	0	0		17.2	8.5	14.9	−3.30	0.676	0.326
231	**5b**[l]	0.998	0.211[j]	0	0		14.4	8.8	32.1	−3.64	0.785	0.547
177-1	**6**[m]	0.989	0.211[j]	3.42	0.221	5.8[n]	5.5	4.6	5.2	−3.92	0.810	0.122
177-2	**6**	2nd precipitation of sample			0.159		6.0	4.0	4.3	−5.58	1.35	0.201
177-3	**6**	3rd precipitation of sample			0.150		6.0					

[a] Mole ratio. [b] Determined by ^{1}H NMR from $n/m = A/10B$, where B was the integral of the signal for $COOCH_2$ (triplet at δ 4.05, 4H) and A was that for 30C10 (singlet at δ 3.65, 40H) ($CDCl_3$). Average of at least two independent integrations. Estimated error, ±0.007. [c] Determined by $\bar{M}_n = [340(B/A) + 2(285) - 168$, where A was the integral of the signal of the blocking group (s, δ 3.72, CH_2, 4H) and B was the signal for the polyester (triplet at δ 4.05; $COOCH_2$, 4H), assuming that both ends of the macromolecule contained the triarylmethyl moieties. Estimated error, ±10%. [d] Determined by measuring the absorption of a known weight of polymer and comparing it to a calibration curve constructed from absorption of known concentrations of methyl 3,3,3-triphenylpropionate in THF at 260 nm. Estimated experimental error, ±2%. [e] Absolute values determined by GPC in THF using a differential viscosity detector. [f] By GPC in THF using a differential viscosity detector. [g] Here, 4.74 mmol of diol in 10 mL of diglyme was heated at 90–100 °C under N_2 flow for 40–45 h. BG, if any, was then added. Reaction mixture was then heated 4 h more. [h] As in footnote *g* but with 9.5 mmol of pyridine. [i] As in footnote *g* except 18 h at 120 °C. [j] BG = $(C_6H_5)_3CCH_2COCl$. [k] As in footnote *g* except 16 h at 90–100 °C prior to BG addition. [l] As in footnote *g* except 18 h at 115 °C. [m] Diol, diacid chloride, and macrocycle were heated at 90–100 °C under N_2 flow for 40 h. BG was added. Reaction mixture was then heated 4 h more. [n] Determined by $\bar{M}_n = (15B/2A)[340 + 440(m/n)] + 2(285) - 168$, where A was the integral of the signal of the blocking group (δ 7.1–7.2, Ar–H, 30H) and B was that of the polyester (triplet, δ 4.05, $COOCH_2$, 4H). Estimated error, ±5%.

as a model for the crown ethers as solvents. This produced poly(decamethylene sebacate) (**5a**). Next, end-capping experiments were performed under similar conditions (Table 1, samples 161, 187, 203, and 231). Addition of 3,3,3-triphenylpropionyl chloride after the esterification had produced hydroxy-terminated polymer led to end-capped polyester samples **5b**.

A 202 mg sample of the poly(decamethylene sebacate) (**5a**) ($\bar{M}_n$ = 7.7, $\bar{M}_w$ = 13 kg/mol) was stirred with 10.5 g (23.9 mmol) of 30-crown-10 (**1**) in the melt at 87 °C for 18 h, dissolved in CH_2Cl_2, and precipitated once into ethanol. The recovered (84%) polymer contained *no* macrocycle as determined by ^{1}H NMR. When the experiment was repeated with 3,3,3-triphenylpropionyl chloride added at the end and the mixture heated an additional 2 h prior to dissolution and precipitation, again the solid contained *no* 30-crown-10 (**1**). These results are important because they demonstrate that (1) large amounts of unthreaded macrocycle are easily removed from the polyester by this precipitation technique and (2) the threading of macrocycles by even modest molecular weight polymers is very slow and inefficient due to the limited number and diffusion rate of chain ends.

B. Polyrotaxane Synthesis. Our first polyester rotaxane was synthesized through the condensation polymerization of sebacoyl chloride (1.00 equiv) with 1,10-decanediol (1.01 equiv) in the presence of 30-crown-10 (**1**) (3.42 equiv), followed by treatment with 3,3,3-triphenylpropionyl chloride (Scheme 1); an end-capped polyester, **6**, was obtained. In this reaction, a slight excess of diol was used to ensure that the polymer chains formed initially were hydroxyl terminated. From the literature,[8] it appeared that a trityl group might be large enough to block 30-crown-10 (**1**); therefore, the commercially available 3,3,3-triphenylpropionyl chloride was selected as the blocking group.

C. Purification and Structure Determination. To isolate polyrotaxane **6** from the unthreaded 30-crown-10 (**1**), we dissolved the polymeric material in chloroform, which is a good solvent for both the polyester and the crown ether, and carried out precipitations into methanol, which dissolves only the crown ether and not the polymer. This was verified by evaporation of the first precipitant solution after filtration; only 30-crown-10 was present as determined by NMR. The second precipitant solution contained 30-crown-10 and <1% polyester.

In the ^{1}H NMR spectrum of poly(decamethylene sebacate) (**5b**) (Figure 2a), the central eight protons of the sebacoyl unit and the central 12 protons of the diol moiety appear at δ 1.3 (labeled a). The signal at δ 1.6 (b) includes the eight protons β to both the carbonyl and the ether oxygen atoms. The four protons α to the carbonyl group appear at δ 2.3 (c). The OCH_2 protons appear as a four proton triplet at δ 4.05 (d). Blocking group signals occur at δ 3.72 (CH_2, e) and δ 7.1−7.2 (f).

The only difference between the spectra of **5b** and **6** is the presence of the signal for the crown ether at δ 3.7 (e) in **6** (Figure 2b). The chemical shifts for the polyester backbone were not affected by the threaded macrocycle; neither was the chemical shift of 30C10 altered by threading. Similar results have been reported for other crown ether-based polyrotaxanes,[24,25] in contrast to systems involving strong attractive interactions between the linear and cyclic components.[11−16,20,21,23]

The composition of the precipitate was analyzed from the integration ratios. Because there are 40 protons per crown ether molecule, estimation of *m/n*, the number of moles of cyclic per repeat unit, can be done quite precisely by comparison of the integrals for 30C1O (singlet, δ 3.67, e) and the OCH_2 signal (triplet, δ 4.05, d) for four protons per repeat unit (Figure 2b). Thus, at *m/n* = 1.0, this integral ratio would be 10, and at *m/n* = 0.10, it would be 1.0.

In this case we found that, within experimental error, the composition of polyrotaxane **6** reached a constant level after two reprecipitations (Table 1, sample 177, last three entries). The final value (*m/n* = 0.150) corresponds to 16 wt % 30-crown-10, or one macrocycle per 147 backbone atoms.

D. Molecular Weights: Polyrotaxane Purity, Mark−Houwink Constants. The UV absorption of poly(decamethylene sebacate) (**5a**) is essentially restricted to short wavelengths. On the other hand, the aromatic moieties of the trityl end-blocking groups absorb strongly. As a model compound, methyl 3,3,3-triphenylpropionate was made; it has a λ_{max} at 260 nm ($\pi \rightarrow \pi^*$) with ϵ = 774. Therefore, quantitative UV analysis enables determination of the weight fraction of blocking groups present in polyester **5b** and polyrotaxane **6**. Then, assuming 100% end-capping, $\bar{M}_n$ can be calculated (Table 1).

^{1}H NMR spectroscopy was also employed to estimate $\bar{M}_n$ in the case of end-blocked model polyester **5b**. This was done in two different ways. The first method utilized the singlet at δ 3.72 (e) due to the methylene protons α to the carbonyl moiety of the blocking groups and the triplet at δ 4.05 (d) due to the OCH_2 protons of the polyester (see Figure 2a). The number average degree of polymerization was calculated as being equal to the ratio of integrals of the δ 4.05 to δ 3.72 signals, $\bar{n} + 1 = I_{4.05}/I_{3.72}$, under the assumption of 100% end-blocking. Alternatively, the aromatic signal of the blocking group (δ 7.1−7.2, f) was utilized. Again assuming 100% end-blocking, the number average degree of polymerization was taken as $\bar{n} + 1 = 15$ ($I_{4.05}/2I_{7.1-7.2}$). The latter method was also applied to estimate $\bar{n}$ for **6**; the former method could not be applied because the δ 3.72 signal of the methylene protons of the blocking group was obscured by the crown ether signal (see Figure 2b). The $\bar{M}_n$ values were calculated by taking into account the end groups and the fact that there is one less sebacoyl moiety than indicated by $\bar{n}$.

Absolute molecular weights of polymers **5a**, **5b**, and **6** were measured by GPC using a viscosity detector and the universal calibration, which relates the elution volume to the product $[\eta][m]$. These results then allow calculation of the Mark−Houwink constants K and a from the relationship $[\eta] = KM^a$, where M is the viscosity average molecular weight. All of these results are summarized in Table 1.

Poly(decamethylene sebacate) (**5a**) had $\bar{M}_n \sim 7-8$ kg/mol and $\bar{M}_w \sim 13-28$ kg/mol (Figure 3a). The average log K and a values (Mark−Houwink) were -2.81 ± 0.18 and 0.575 ± 0.045, respectively. Polyester samples **5b** were incompletely end-capped, as deduced from comparison of $\bar{M}_n$ values determined by absolute GPC, NMR, and UV end group analyses. $\bar{M}_n$ values derived from end group analysis assuming two end groups per macromolecule gave values that were 39−283% higher than GPC values for several end-capping conditions. These results indicated that end-capping ranged from 26 to 71% complete. $\bar{M}_n$ ranged from 7 to 9 kg/mol, and $\bar{M}_w$ from 12 to 32 kg/mol. It is interesting to note that for end-capped polyester samples **5b**, the average values for log K and a were -3.47 ± 0.20 and 0.731 ± 0.058, respectively; these represent changes relative to the simple polyester itself, **5a**, ascribable to the rigid trityl end groups.

A comparison of the $\bar{M}_n$ value of polyrotaxane **6** determined by UV end group analysis with the GPC result (Table 1) indicates that 77% end-capping was achieved, i.e., assuming that there are no non-end-capped chains, 46% of the macromolecules have only one end cap and 54% have two end caps. NMR data gave similar conclusions. Furthermore, experiments with molecular models indicate that the trityl group is not large enough to prevent loss of 30-crown-10 (**1**) by dethreading. The

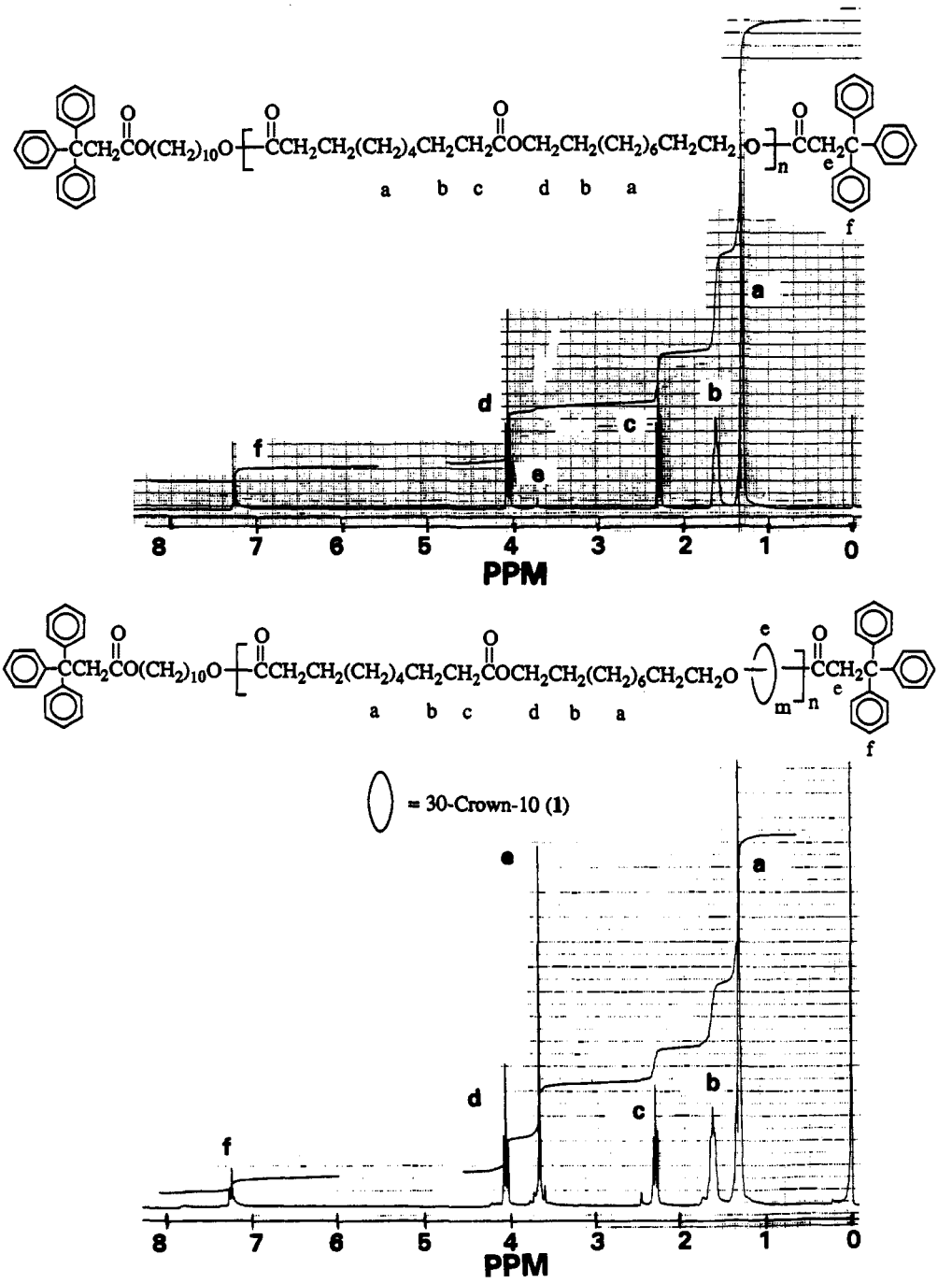

Figure 2. 270 MHz ^{1}H NMR spectra of (a, top) poly(decamethylene sebacate) (**5b**) (sample 161) and (b, bottom) poly[(decamethylene sebacate)-rotaxa-(30-crown-10)] (**6**) (Table 1, sample 177-3) in $CDCl_3$. The singlet at δ 3.67 (**e**, bottom) is due to the macrocycle. $CHCl_3$ appears at δ 7.35.

loss of macrocycle in the second precipitation indeed seems to be the result of dethreading of crown ether molecules near the chain ends in solution, inasmuch as sample 177-1 showed no free crown by TLC. However, since the GPC trace of the polyrotaxane (Figure 3b) after the second precipitation does not reveal any free 30-crown-10 (M = 440), it appears that dethreading, even for low molecular weight ($\bar{M}_n$ = 4 kg/mol corresponds to $\bar{n} \cong 12$) polymers does not occur on the time scale of GPC elution. This sample (177-2) had 1.6 macrocycles per macromolecule. Elsewhere we reported that solutions of these samples do show a reduction in viscosity over a period of several weeks, indicating perhaps a slow dethreading process,[31] but also perhaps hydrolytic degradation of the backbone. Random coiling of the backbone apparently traps the macrocycle in chain folds for extended periods of time.

Finally, the log K and a values for the polyrotaxane after the second precipitation must be noted: −5.58 and 1.35, respectively. Compared to the end-capped polyester **5b** (sample 161, 72%, end-capped log K = 3.70, a = 0.793), these values represent a change in K of 2 orders of magnitude and almost a doubling of a! Interpretation of these results is complicated by the probable change in solubility parameter as a result of rotaxane formation, but nonetheless it appears that rotaxanes made from relatively small macrocycles may cause stiffening of the polymer backbone (increasing a).

E. Thermal Properties. The end-blocked polyester **5b** (Table 1, sample 161) displayed a melting temperature (T_m) of 73 °C; a sample of non-end-blocked polyester **5a** (Table 1, sample 157) had T_m = 76 °C. Reported T_m values range from

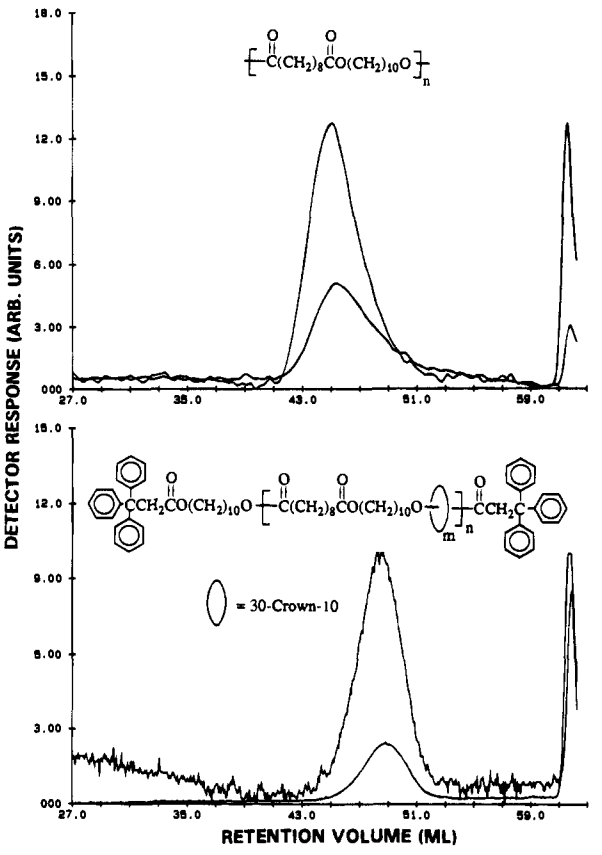

Figure 3. Gel permeation chromatography traces for (a, top) poly(decamethylene sebacate) (**5a**) (sample 157) and (b, bottom) poly[(decamethylene sebacate)-rotaxa-(30-crown-10)] (**6**) (sample 177-3) in THF at 30 °C, high intensity curves, viscosity detector; low intensity curves, refractive index detector.

71 to 78 °C.[32-36] The polyrotaxane **6** (Table 1, sample 177) after the first precipitation had T_m = 58 °C, after the second precipitation T_m = 69 °C, and after the third precipitation T_m = 69 °C. Thus the presence of the 30-crown-10 (**1**) in the polyrotaxane lowers T_m, but only a few degrees. There are insufficient data to correlate this depression with crown ether content and hence estimate a Flory χ value. Because of the high crystallinity of these polyesters, the glass transition temperature, T_g, could not be detected by DSC.

Although this synthesis was simple and straightforward and the results were encouraging and intriguing, we found that the molecular weight of polyrotaxane **6** was lower than that of polymer **5b**, the model polymer, and we believed this was caused by the offset of the stoichiometry of the reactants. It is well known that a small deviation from the desired stoichiometry in polycondensation will lower the molecular weight of the polymer significantly; unfortunately, it is difficult to achieve a precise stoichiometry in this reaction, particularly in small-scale syntheses, since 30-crown-10 (**1**) may contain a small amount of poly(ethylene glycol), unless it is carefully purified.[28] In these early experiments, the 30-crown-10 employed was not as highly pure as that used in the work described below. Furthermore, incomplete end-capping had been encountered. To eliminate these problems, we continued our synthetic program using transesterification polymerization techniques.

(32) Korshak, V. V.; Vinogradova, S. V.; Vlasova, E. S. *Dokl. Akad. Nauk SSSR* **1954**, *94*, 61.
(33) Mayer, R. *Bull. Soc. Chim. Fr.* **1966**, 2998.
(34) Howard, G. J.; Knutton, S. *Polymer* **1968**, *9*, 527.
(35) Woo, E. M.; Barlow, J. W.; Paul, D. R. *Polymer* **1985**, *26*, 763.
(36) Fernandes, A. C.; Barlow, J. W.; Paul, D. R. *Polymer* **1986**, *27*, 1799.

II. Diester/Diol Transesterification Polymerizations: Poly(triethyleneoxysebacate) and Poly(1,4-butylene sebacate) Rotaxanes (11–20). Transesterification, a widely used procedure in polyester synthesis referred to as ester interchange or alcoholysis, was adopted as the alternate synthesis method for polyester rotaxanes. This approach has two advantages over the earlier one. Firstly, it does not require very precise stoichiometry. Secondly, the requirement on the purity of macrocycle is lowered, too, because the trace amount of poly(ethylene glycol) that may exist in 30-crown-10 does not influence the polymerization by upsetting the stoichiometry, providing that the major diol is relatively more volatile.

Due to the fact that the supply of crown ethers was initially limited, it was desirable to use a low molar ratio of the macrocycle and the diester in the starting materials. It was believed that when the polymer backbone possessed structural units similar to that of the macrocycle, better threading percentages might be achieved due to the more favorable interaction. Tri(ethylene glycol) was used as the first diol in this investigation, based on this concern.

The model polyester **7a** was synthesized from the condensation polymerization of dimethyl sebacate and tri(ethylene glycol) with the use of a variety of catalysts. Problems with metallic transesterification catalysts such as manganese or cadium acetate or antimony oxide were anticipated and observed, because of the strong complexing capabilities of the crown ethers. Among the transesterification catalysts tested, *p*-toluenesulfonic acid appeared to be the most effective one; therefore, it was used as the standard catalyst for all the polymerizations reported here.

In order to choose the reaction temperatures, the thermal stabilities of the crown ethers were examined by thermogravimetric analyses (TGAs). The 5% weight losses of 30–60-membered crown ethers occurred at temperatures ranging from 205 to 214 °C in air and from 265 to 376 °C in nitrogen.[28] For this reason, initial polymerizations were carried out at 180 °C. While poly(butylene sebacate) and its rotaxane counterparts with high molecular weights were successfully synthesized under these conditions, we did not obtain poly(triethyleneoxy sebacate) and the corresponding polyrotaxanes at 180 °C due to the high boiling point of tri(ethylene glycol). It is obvious that the polycondensation reactions for the synthesis of poly(triethyleneoxy sebacate) rotaxanes should be carried out at temperatures higher than the onset decomposition temperatures of the crown ethers.

Two questions were related to this problem. First, is the onset of mass loss of crown ethers observed by TGA due to volatilization or decomposition? Second, are crown ethers more stable under high vacuum conditions of the polycondensation reactions than in air or nitrogen because of the absence of the oxygen? A study was performed to examine the thermal stability of crown ethers under the conditions for the polymerization. In the presence of a trace amount of *p*-toluenesulfonic acid under vacuum, 42C14 was heated at 240 °C. The sample was then analyzed by melting point measurement, ^{1}H NMR, and ^{13}C NMR. The sample had the same melting point as standard 42C14. Both ^{1}H and ^{13}C NMR spectra showed only pure 42C14 peaks. The analytical results demonstrate that 42C14 does not decompose under the test conditions.

Poly(butylene sebacate) was also prepared at 180 °C in the presence of 18-crown-6, which is impossible to threaded onto the polymer backbones because of its small cavity. The ^{1}H NMR spectrum of the product did not show any evidence of extraneous signals. It can be concluded that 18C6 does not decompose under polymerization conditions and is not incorporated into the polyester in any way. Some 18C6 was lost

Scheme 2

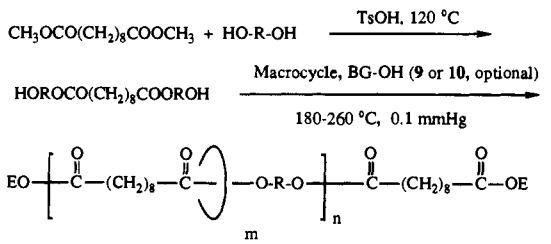

7a: R = $(CH_2CH_2O)_2CHCH_2$, $\frac{m}{n}$ = 0, E = H
7b: R = $(CH_2CH_2O)_2CHCH_2$, $\frac{m}{n}$ = 0, E = BG (**9**)
8a: R = $-(CH_2)_4-$, $\frac{m}{n}$ = 0, E = H
8b: R = $-(CH_2)_4-$, $\frac{m}{n}$ = 0, E = BG (**10**)
11a: R = $-(CH_2CH_2O)_2CH_2CH_2-$, ⟨⟩ = 1, E = H
11b: R = $-(CH_2CH_2O)_2CH_2CH_2-$, ⟨⟩ = 1, E = BG (**9**)
11c: R = $-(CH_2CH_2O)_2CH_2CH_2-$, ⟨⟩ = 1, E = BG (**10**)
12: R = $-(CH_2CH_2O)_2CH_2CH_2-$, ⟨⟩ = 3, E = H
13: R = $-(CH_2CH_2O)_2CH_2CH_2-$, ⟨⟩ = 4, E = H
14: R = $-(CH_2)_4-$, ⟨⟩ = 1, E = H
15: R = $-(CH_2)_4-$, ⟨⟩ = 2, E = H
16: R = $-(CH_2)_4-$, ⟨⟩ = 3, E = H
17a: R = $-(CH_2)_4-$, ⟨⟩ = 4, E = H
17b: R = $-(CH_2)_4-$, ⟨⟩ = 4, E = BG (**9**)

through distillation, however. Thus, some loss of the larger crown ethers by volatilization may occur, but in a view of their much higher boiling points, it is expected to be minimal.

Based upon the results of this study, the polycondensation reactions for synthesis of poly(triethyleneoxy sebacate) rotaxanes were carried out at 200−260 °C.

A. Synthesis and Purification. 1. Model Linear Systems: Poly(triethyleneoxy sebacate) and Poly(butylene sebacate). The model polymers, poly(triethyleneoxy sebacate) (**7a**) and poly(butylene sebacate) and (**8a**), were synthesized from the condensation polymerization of dimethyl sebacate with tri(ethylene glycol) and with 1,4-butanediol, respectively (Scheme 2). In a typical polymerization, 1.0 equiv of dimethyl sebacate, 2.2 equiv of diol, and 0.01 equiv of *p*-toluenesulfonic acid (transesterification catalyst) were mixed and heated at 120−150 °C under nitrogen to allow the initial transesterification reaction to occur as shown in Scheme 2. The system was then heated to 180−200 °C (for **8**) or 200−260 °C (for **7**) gradually under 0.1 mmHg vacuum, and the polycondensation was allowed to proceed for 6−30 h. Excess diol was removed during this period. In the case of 1,4-butanediol, transesterification at the higher temperature has the advantage of producing tetrahydrofuran and water under the influence of the acidic catalyst. This enables the esterification equilibrium to be driven toward completion at relatively low temperatures.

The end-blocked model polymers **7b** and **8b** were made by inclusion of triarylmethyl derivatives bearing a hydroxy functionality in the reaction mixture. For these experiments, instead of the trityl-based derivatives, larger blocking groups were used: 4,4-bis(*p*-*tert*-butylphenyl)-4-phenylbutanol (**9**) or 2-{2-[*p*-(tris-*p*-*tert*-butylphenyl)methyl)phenoxy]ethoxy}ethanol (**10**). Both blocking groups are large enough to prevent loss of 30-crown-10 (**1**) or BPP (**4**), and **10** is large enough to constrain 42-crown-14 (**2**), while **9** is not; neither **9** nor **10** is large enough

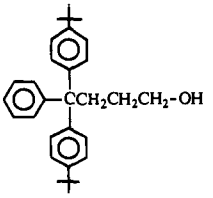

9 (BG-OH)

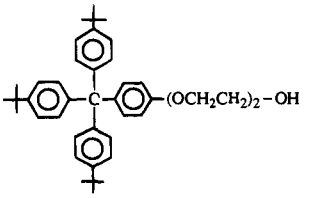

10 (BG-OH)

to block 60-crown-20 (**3**), as deduced from CPK models. The syntheses of **9** and **10** are reported elsewhere.[37]

Model diester **18** was synthesized from blocking group alcohol **9** and sebacoyl chloride. Its ^{1}H NMR spectrum is shown in Figure 4, and the signals are identified as being due to various protons in the structure. The spectrum of this compound aids in analysis of the polyrotaxane spectra.

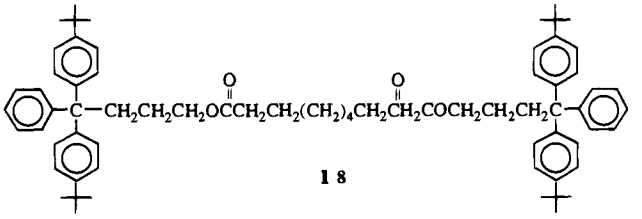

18

2. Polyrotaxanes. The polyester rotaxanes **11**−**17** were synthesized similarly, except that the condensation step was carried out in the presence of one of the macrocycles (Scheme 2).

In order to prove that polyrotaxanes were produced, a protocol for purification and analysis was developed. Purification consisted of multiple reprecipitations into a good solvent for the macrocycle. After each precipitation, the composition of the dried solid was determined by quantitative ^{1}H (and ^{13}C) NMR spectroscopy, affording a measure of the molar ratio of macrocycle to repeat units (*m*/*n*). Once constant composition was achieved, the absence of unthreaded macrocycles was demonstrated by gel permeation chromatography, which also provided the molecular weights.

(a) Poly(triethyleneoxy sebacate) Rotaxanes. The ^{1}H and ^{13}C NMR spectra of end-capped poly(triethyleneoxy sebacate) (**7b**, sample 141) are shown in Figures 5a and 6a. The ^{1}H NMR spectrum contains signals as follows: δ 1.3 (labeled a), a broad peak for the eight "central" protons of the sebacoyl moiety and the methyl protons of the blocking groups; δ 1.65 (b), a triplet for the four methylene protons β to the carbonyl groups; δ 2.35 (c), a triplet for the four protons α to the carbonyl group; δ 3.6−3.7 (e), a complex signal for the eight central ethyleneoxy protons; δ 4.25 (d), a triplet for the four protons of the $COOCH_2$ moieties; δ 7.15−7.35 (f), a multiplet for the aromatic protons of the blocking groups (**9**). Careful inspection reveals other very small signals from the end-blocking groups; refer to Figure 4.

The ^{13}C NMR spectrum of **7b** (Figure 6a) contains seven peaks in total. Only three peaks (a,b,c) at δ 24−35 are observed for the four distinct CH_2 carbons of the sebacoyl unit, but all three signals (δ 63−72, e,f,g) appear for the three nonequivalent ethyleneoxy carbons. The carbonyl C is observed at δ 174 (d). The end groups are not observed at this attenuation.

The spectra for the 30-crown-10-based polyrotaxane **11b** (sample 144) are shown in Figures 5b and 6b. The only difference in the proton spectrum of **11b** relative to **7b**, apart from a different end-blocking group content, is an enhancement

(37) Gibson, H. W.; Lee, S. H.; Engen, P. T.; Lecavalier, P.; Sze, J.; Shen, Y. X.; Bheda, M. *J. Org. Chem.* **1993**, *58*, 3748.

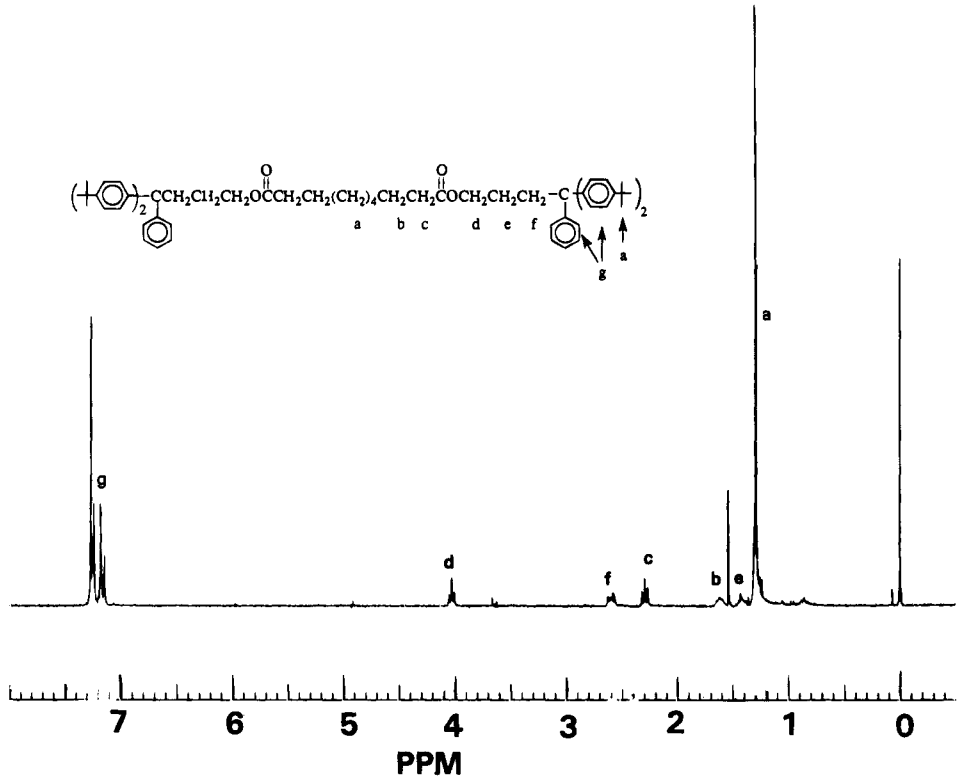

Figure 4. 270 MHz ^{1}H NMR spectrum of di[4,4-bis(*p-tert*-butylphenyl)-4-phenylbutyl] sebacate (**18**) in $CDCl_3$.

of the cluster at δ 3.6−3.7 (e) because of the crown ether singlet at δ 3.67. Likewise, in the carbon spectrum, the only change is an increase in the intensity of the signal at δ 70.7 (g). As in **6**, no chemical shift changes result from rotaxane formation.

The cyclic content (*m/n*) was determined by integration of the ^{1}H NMR signals from δ 3.5 to 3.8 (e) versus δ 4.1 to 4.4 (d). The former peaks (e) contain the crown ether protons and the central eight protons of the triethyleneoxy moiety, while the d signal corresponds to the four protons α to the carbonyl group. Because 30-crown-10 contains 40 protons per molecule, the precision of the *m/n* determination is high. For *m/n* = 1, the e/d ratio would be 48/4 = 12; for *m/n* = 0.1, e/d would be 1.2. In this case (Figure 5b), *m/n* was 0.23.

Table 2 shows a systematic study of the macrocycle content in the poly(triethylene sebacate) rotaxanes **11**−**13** after each reprecipitation. Sample 149 is the control experiment, which shows the reprecipitation result of a blend of poly(triethyleneoxy sebacate) (**7a**) and 30-crown-10 (**1**). The blend was prepared by evaporating solvent from a CH_2Cl_2 solution of the two components and then heating them in the melt at 100 °C for 48 h. After the first and second reprecipitations, the *n/m* ratio reached 16 and 23, respectively, indicating that the majority of free macrocycle can be removed easily. When the material obtained from the second precipitation was kept in solution for 3 days before the third reprecipitation was carried out to provide sufficient time for the disentanglement of polymer chains and macrocycles, no 30-crown-10 was detected in the precipitate. In this case, 86% of the polyester was recovered. As noted above for a similar experiment with **5a**, these results are important for two reasons: (1) they demonstrate that physical blends of cyclic and linear polymeric components are readily separated by reprecipitation methods and (2) the threading of preformed polymers, even of modest molecular weights, is a slow and inefficient process.

In contrast, poly[(triethyleneoxy sebacate)-rotaxa-(30-crown-10)][30] with end-blocking groups (polymer **11b**, Table 2, sample 2) had a ratio of repeating units to 30-crown-10 [*i.e.*, *n/m*] of 4.2 after the first precipitation. This ratio did not change significantly upon the second and the third reprecipitations, indicating that a stable composition had been reached. This corresponds to a macrocycle content of 24% by weight in the polyrotaxane. If the same polymer (**11b**) was allowed to stay in solution for a period of 3−5 days before each precipitation was carried out, a slightly higher *n/m* ratio (5.1) was obtained (Table 2, sample 3), presumably due to less than quantitative end-blocking (see below), thus allowing macrocycles near chain ends to diffuse off the backbone. The loss amounted to 3 mass %. Indeed, NMR analysis indicates that less than complete end-blocking was achieved in general as discussed below. However, after the first precipitation, further reprecipitations did not change this ratio. Thus, polymer **11b** is not a simple physical blend of polymer **7b** and 30-crown-10 (**1**), but a stable copolymer of the two, i.e., a polyrotaxane.

Indeed, the macrocycle content of polyrotaxane **11a** *without* end-blocking groups after purification (sample 4), *n/m* = 5.2−5.6 or 20−21 mass %, was nearly the same as for polyrotaxane **11b** (sample 3) whether the reprecipitations were carried out immediately after dissolution or 3−5 days later (samples 4, 230, and 146). However, synthesis of polyrotaxane **11c** (sample SL-2-34) using the larger blocking group **10** increased the 30-crown-10 content to *n/m* = 3.2 (30 mass %) in spite of lower molecular weight and incomplete end-capping (see below).

Poly(triethyleneoxy sebacate) rotaxanes **12** and **13**, incorporating 60-crown-20 (**3**) and bis(p-phenylene)-34-crown-10 (**4**), respectively, were analogously produced, purified, and analyzed, as shown in Table 2.

The ^{1}H and ^{13}C NMR spectra of poly[(triethyleneoxy sebacate)-rotaxa-(60-crown-10)] (**12**) are qualitatively similar to those of the 30-crown-10 analogs **11** shown in Figures 5 and 6. The only differences are small differences in chemical shifts and the relative intensities of the crown ether signals.

(b) Poly(butylene sebacate) Rotaxanes. Polyrotaxanes **14**−**17** comprised of poly(butylene sebacate) backbones and 30-crown-10 (**1**), 42-crown-14 (**2**), 60-crown-20 (**3**), and bis(*p*-

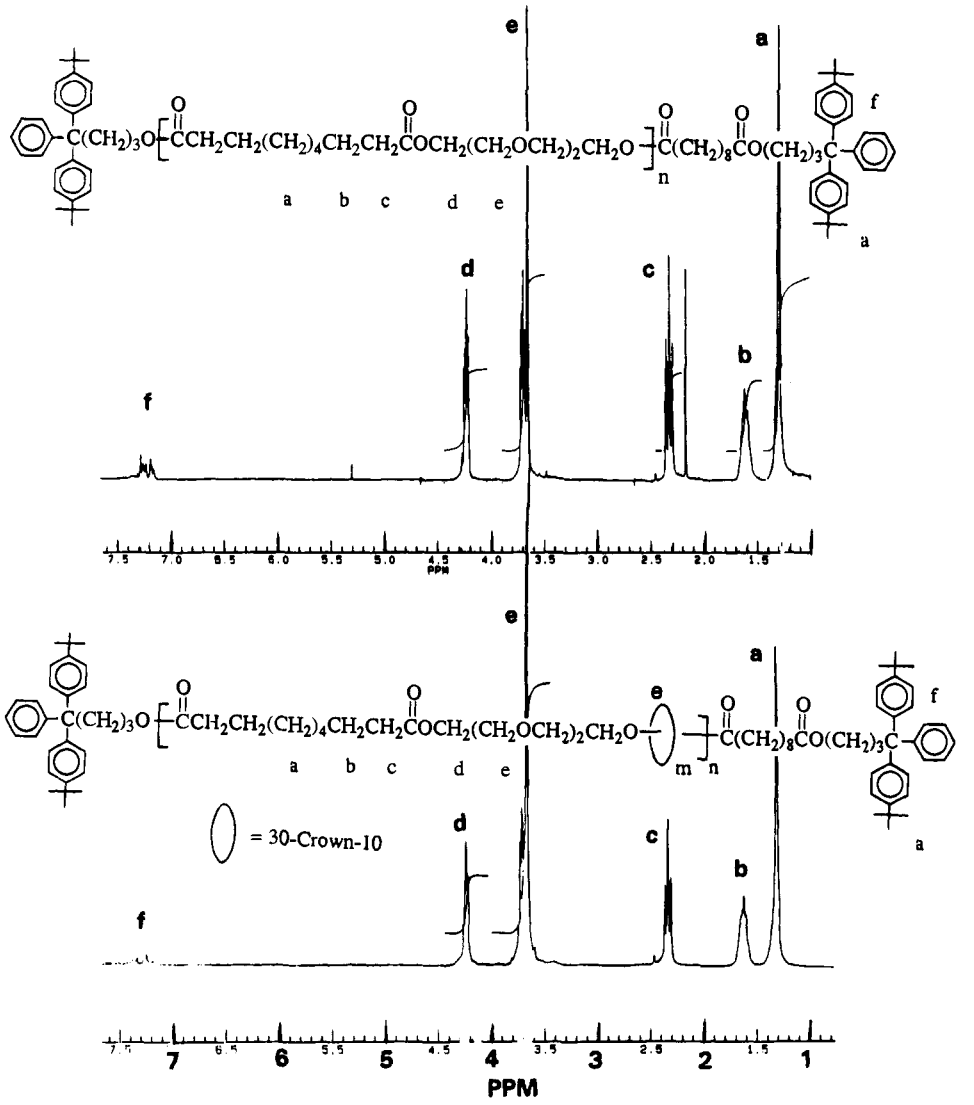

Figure 5. 270 MHz ^{1}H NMR spectra of (a, top) end-blocked poly(triethyleneoxy sebacate) (**7b**) and (b, bottom) end-blocked poly[(triethyleneoxy sebacate)-rotaxa-(30-crown-10)] (**11b**) in $CDCl_3$. The large peak at δ 2.15 (top) is due to CH_3COCH_3. The small peak at δ 5.3 (top) is due to CH_2Cl_2.

phenylene)-34-crown-10 (**4**, BPP) respectively, were prepared, purified, and analyzed in analogous fashion. The results are summarized in Table 3.

The ^{1}H NMR spectra of poly(butylene sebacate) (**8a**) and poly[(butylene sebacate)-rotaxa-(42-crown-14)] (**15**) are shown in Figure 7. The polyester **8a** displays resonances at δ 1.3 (labeled a) for the central $(CH_2)_4$ unit (8H) of the sebacoyl moiety, at δ 1.6 (b) for the $COCCH_2$ protons (4H), at δ 1.7 (e) for the $OCCH_2$ protons (4H), at δ 2.3 (c) for the $COCH_2$ group (4H), and at δ 4.1 (d) for the OCH_2 protons (4H).

The ^{1}H NMR spectrum of **15** contains only one additional peak at δ 3.7 (f) due to the crown ether. As observed with polyrotaxanes **11** and **12**, there are no changes in chemical shifts in the polyrotaxane relative to the two individual components. With butylene sebacate polymers, integration of the δ 3.7 (f) peak (56H in the case of **2**, Figure 7b) directly versus the integrals of the peaks for all the "internal" protons from δ 1.2 to 1.9 (a,b,e, 16H) yields *m/n*. For **15**, then, $m/n = 1$ would yield an integral ratio [f/(a + b + e)] of 56/16 = 3.5; again, composition can be determined with good precision because of the large number of protons in the crown ether.

30-Crown-10- and 60-crown-20-based poly(butylene sebacate)s **14** and **16** afforded qualitatively identical spectra relative to **15** (Figure 7b). Only the relative intensities of the crown ether signals at δ 3.7 varied.

The ^{13}C NMR spectra of poly(butylene sebacate) (**8a**) and poly[(butylene sebacate)-rotaxa-(60-crown-20)] (**16**) are shown in Figure 8. **8a** displays six of a possible seven signals. Apparently the four central carbon atoms of the sebacoyl unit are indistinguishable, as they were in **7b** (Figure 6); these are assigned to the upfield signal at δ 24.8 (labeled a). The two equivalent central carbons of the diol moiety are assigned as the δ 25.3 signal (f). Carbons β to the carbonyl are designated as giving rise to the δ 29.0 signal (b) and those α to the carbonyl the δ 34.2 signal (c). The carbons α to the ether oxygen are responsible for the δ 63.6 peak (e), and the carbonyl carbon is observed at δ 173.7 (d).

The ^{13}C NMR spectrum of polyrotaxane **16** (Figure 8b) differs from that of the model polymer **8a** only by the resonance at δ 70.5 (g), easily assigned to the carbons of the 60-crown-20 component of the polyrotaxane.

The ^{1}H NMR spectrum of bis(*p*-phenylene)-34-crown-10 (BPP) (**4**) is shown in Figure 9. The spectra of poly[(butylene sebacate)-rotaxa-(bis-*p*-phenylene)-34-crown-10)] (**17a**) after the first and second precipitations are shown in Figure 10. The polyester backbone resonances of **17a** (Figure 10) match those

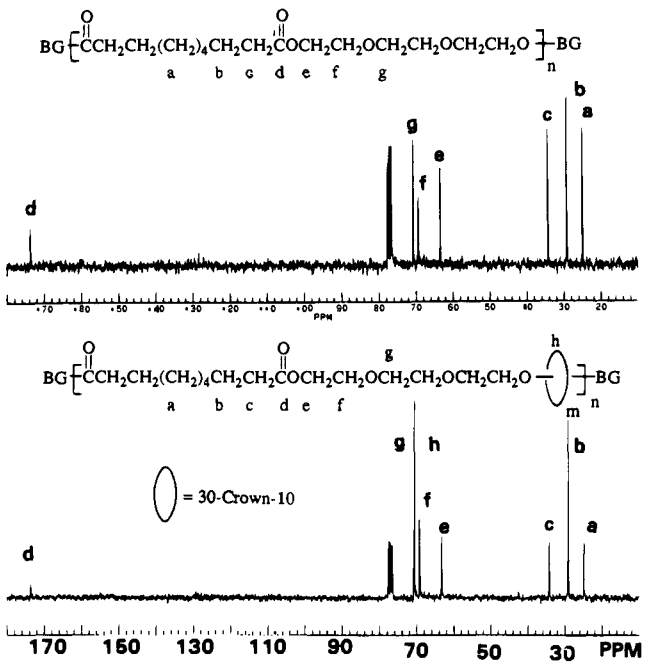

Figure 6. 68 MHz ^{13}C NMR spectra of (a, top) poly(triethyleneoxy sebacate) (**7b**) and (b, bottom) poly[(triethyleneoxy sebacate)-rotaxa-(30-crown-10)] (**11b**) in $CDCl_3$. The three peaks at δ 77 are due to $CDCl_3$. Blocking group signals are not observed at this attenuation.

of poly(butylene sebacate) (**8a**, Figure 7a). However, contrary to observations with the other crown ethers, note that in the first precipitate two signals were observed for the aromatic protons of **4**, suggesting that one corresponded to unthreaded or free **4** and the other resulted from the cyclic component of polyrotaxane **17a**. The upfield signal (δ 6.75) had the same chemical shift as seen in pure BPP (**4**) (Figure 9). Indeed, in subsequent precipitations this signal disappears, leaving only the δ 6.85 signal. Similar results were obtained with **17b**; the δ 6.75 signal was observed only in the first precipitate.

We believe that it is the prohibition of the rotation of the phenylene rings in the polyrotaxane which causes the downfield shift. In the unthreaded macrocycle, the edge-on-face conformation brought about by this rotational process causes shielding of the aromatic protons.

It is noteworthy that the ethyleneoxy signals of the crown ether also shift upfield in the polyrotaxane; the signal at δ 4.0 that is present in BPP (Figure 9) and in the polymer after the first precipitation (Figure 10a) does not appear in the polyrotaxane after the second precipitation (Figure 10b). Therefore, this macrocycle, BPP, because of differences between the chemical shifts of various signals for the threaded and free or unthreaded species, allows the NMR technique to be used as a measure of purity as well as composition of resulting polyrotaxanes.

B. Proof of Structure. 1. Poly(triethyleneoxy sebacate) Rotaxanes. To confirm the integrity of 30-crown-10 in the polyrotaxanes derived from tri(ethylene glycol), we analyzed the products from the hydrolysis of polyrotaxane **11b**. As expected, when the hydrolysis was conducted under basic conditions (Scheme 3), tri(ethylene glycol) and 30-crown-10 were produced; no glycol other than tri(ethylene glycol) was detected. This proved the integrity of the crown ether in the polyrotaxane.

2. Poly(butylene sebacate) Rotaxanes. At the early stage of the work, attempts to prepare polyrotaxanes were hampered by the small amount of poly(ethylene glycol)s present as impurities in the crown ethers. These poly(ethylene glycol)s were found to copolymerize into the polymer backbones of the polyrotaxanes, leading to a triplet at δ 4.23 and multiplets at δ 3.5−3.8 in the ^1H NMR spectra. The triplet is assigned to OCH_2CH_2OOC and the δ 3.5−3.8 multiplet to the ethyleneoxy protons. Two signals at δ 63.1 and 69.0 in the ^{13}C NMR spectra were also attributed to the poly(ethylene glycol) impurities, CH_2-OOC and CH_2COOC, respectively. Forturnately, we developed a technique to remove poly(ethylene glycol)s by treating the crown ethers with poly(methacryloyl chloride).[28] Utilizing purified crown ethers, we generated polyrotaxanes whose purity was demonstrated by the lack of these impurity-derived signals in both the ^1H and ^{13}C NMR spectra (e.g., see Figures 7b and 8b).

Table 2. Reprecipitation Results for Rotaxanes Based on Poly(triethyleneoxy sebacate), 30-Crown-10, 60-Crown-20, and Bis(*p*-phenylene)-34-Crown-10 via Scheme 2

sample no.	polymer	cyclic	S/M ratio[a]	BGOH used	react condn[b]	reprecipn condn[c]	*n/m* ratio in polymer 1st ppt	2nd ppt	3rd ppt	final backbone atoms per cyclic	final wt % macrocycle
149	blend	30C10	0.91[d]	no		A, B[e]	16[f]	23	∞	0	0
4	**11a**	30C10	0.91	no	I	B[g]	4.8[f]	5.2	5.2	104	21
230	**11a**	30C10	0.91	no	I	A[g]	5.5[f]	5.6		112	20
146	**11a**	30C10	0.92	no	II	A[e]	4.8[f]	5.2		104	21
2	**11b**	30C10	0.91	**9**	II	A[e]	4.2[f]	4.3	4.3	86	24[h]
144	**11b**	30C10	0.91	**9**	II	A[e]	4.0[f]	4.3		86	24[h]
3	**11b**	30C10	0.91	**9**	II	B[e]	4.8[f]	5.0	5.1	102	21[h]
SL-2-34	**11c**	30C10	0.91	**10**	III	A[g]	3.2[f]	3.2	3.2	64	30[h]
222	**12**	60C20	1.81	no	IV	A[g]	1.9[i]	2.2	2.3	46	55
SL-2-25	**12**	60C20	1.81	no	V	A[g]	1.9[i]	2.4	2.4	48	54
212	**13**	BPP	3.48	no	VI	A[e]	18[j]	21	27	540	5.9

[a] S/M was the molar ratio of dimethyl sebacate to macrocycle in the monomer feed. [b] I: 140 °C/N_2, 10 h, 200 °C/0.3 Torr, 30 h. II: 120 °C/N_2, 10 h; 260 °C/0.7 Torr, 6h. III: 120 °C/N_2, 21 h; 260 °C/0.3 Torr, 5 h. IV: 140 °C/N_2, 48 h; 175 °C/0.1 Torr, 16 h; 210 °C/0.1 Torr, 20 h. V: 120 °C/N_2, 12 h; 260 °C/0.2 Torr, 12 h. VI: 140 °C/N_2, 4 h; 210 °C/0.1 Torr, 16 h. [c] Reprecipitation conditions: A, the precipitation was carried out immediately after the polymer was dissolved in the solvent; B, the precipitation was carried out after the polymer solution had been kept for 3−5 days. [d] The content of the blend material was such that the molar ratio of the sebacate unit to macrocycle was 0.91. [e] Sample was dissolved in CH_2Cl_2 and precipitated into ≥20× volume of methanol. Solid was isolated by filtration. [f] Determined by the formula $n/m = [10A/(B - 2A)]$, where A was the integral for signals in the range δ 4.1−4.4 (−$COOCH_2$− of polyester, 4H) and B was the integral for signals in the range δ 3.5−3.9 [all other −OCH_2's of polyester (8H) and crown ether (40H)]. Estimated error, ≤ ±0.1. [g] Sample was dissolved in THF and precipitated into ≥20× volume of water. Solid was isolated by centrifugation followed by filtration. [h] End groups ignored in this calculation: wt % = 440/[440 + (n/m)(316)]. [i] Calculated from $n/m = [20A/(B - 2A)]$, where A and B are defined as in footnote *f*; crown has 80H. Estimated error, ≤±0.1. [j] Calculated from $n/m = A/2B$, where A was the integral for signals in the range δ 1.20−2.40 [$(CH_2)_8$ of sebacate residue (16H)] and B was that for the δ 6.85 signal (8 arom H of **4**). Estimated error, ≤±2.

Table 3. Reprecipitation Results for Rotaxanes Based on Poly(butylene sebacate), 30-Crown-10, 42-Crown-14, 60-Crown-20, and Bis(*p*-phenylene)-34-Crown-10 via Scheme 2

sample no.	polymer	cyclic	S/M ratio[a]	BGOH used	reactn condn[b]	reprecipn condn[c]	*n/m* ratio in polymer 1st ppt	2nd ppt	3rd ppt	final backbone atoms per cyclic	final wt % macrocycle
234	**14**	30C10	0.91	no	I	A[d]	6.5[e]	7.5	7.8	125	18
SL-3-42	**15**	42C14	1.27	no	II	A[d]	4.3[f]	4.4	4.5	73	35
232	**16**	60C20	3.17	no	I	A[g]	4.0[h]	3.8	4.3	69	44
240	**16**	60C20	1.86	no	III	A[g]		3.5[h]		56	50
SL-197	**16**	60C20	1.86	no	IV	A[g]	2.6[h]	3.5	3.3	53	51
196	**17a**	BPP	0.86	no	V	A[d]		17[i]	33	528	6.0
198	**17b**	BPP	1.0	**9**	VI	A[d]		36[i]		576	5.5

[a] S/M was the molar ratio of dimethyl sebacate to macrocycle in the monomer feed. [b] I: 140 °C/N_2, 24 h; 180 °C/0.2 Torr, 30 h. II: 120 °C/N_2, 10 h; 180 °C/0.1 Torr, 20 h. III: 140 °C/N_2, 5h; 195 °C/0.1 Torr, 20 h. IV: 120 °C/N_2, 24 h; 180 °C/0.1 Torr, 24 h. V: 125 °C/N_2, 12 h; 200 °C/0.1 Torr, 20 h. VI: 150 °C/N_2, 4 h; 200 °C/0.1 Torr, 24 h. [c] Reprecipitation conditions: A, the precipitation was carried out immediately after the polymer was dissolved in the solvent. [d] Sample was dissolved in CH_2Cl_2 and precipitated into ≥20× volume of methanol. Solid was isolated by filtration. [e] Calculated from $n/m = 5A/2B$, where A was the integration of signals in the range δ 1.20−1.80 (internal CH_2's of backbone, 16H) and B was that for the δ 3.67 signal for the 40H of **1**. Estimated error, ±0.2. [f] Calculated from the formula $n/m = 7A/2B$, where A was the integration of signals in the range δ 1.20−1.80 (internal CH_2's of backbone, 16H) and B was that for the δ 3.67 signal for the 56H of **2**. Estimated error, ≤ ±0.1. [g] Sample was dissolved in THF and precipitated into ≥20× volume of water. Solid was isolated by centrifugation followed by filtration. [h] Calculated from the formula $n/m = 5A/B$, where A was the integration of signals in the range δ 1.20−1.80 (internal CH_2's of backbone, 16H) and B was that for the δ 3.67 signal for the 80H of **3**. Estimated error, ≤ ±0.1. [i] Calculated from the formula $n/m = A/2B$, where A was the integration of signals in the range δ 1.20−1.80 (internal CH_2's of backbone, 16H) and B was that for the δ 6.85 signal for the 8H (arom) of **4**. Estimated error, ±2. [j] End-blocking groups ignored in this calculation: wt % = $M_{crown}/[M_{crown} + (n/m)256]$, where M_{crown} is the molecular weight of the crown ether.

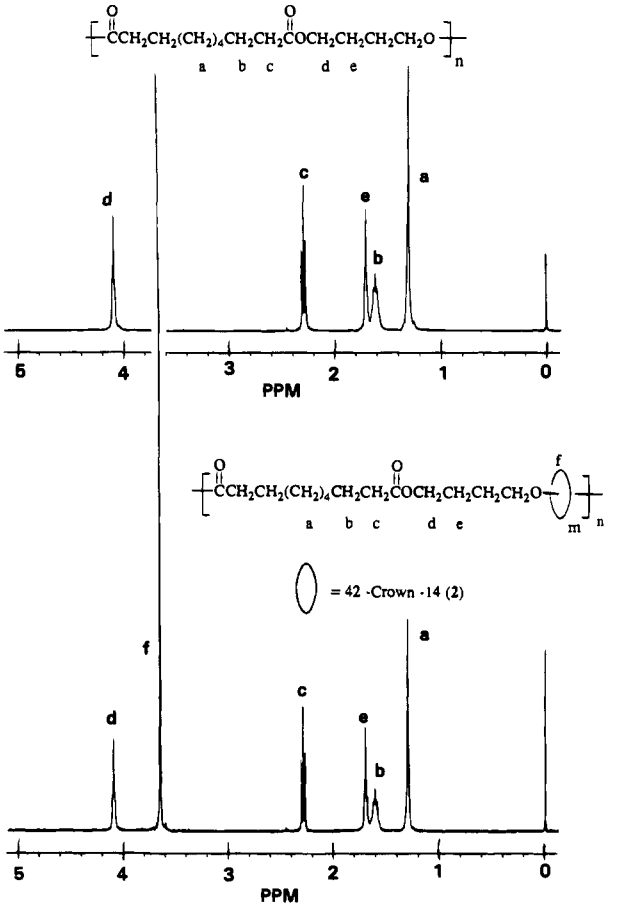

Figure 7. 400 MHz ^{1}H NMR spectra for (a, top) poly(butylene sebacate) (**8a**) and (b, bottom) poly[(butylene sebacate)-rotaxa-(42-crown-14)] (**15**) in $CDCl_3$.

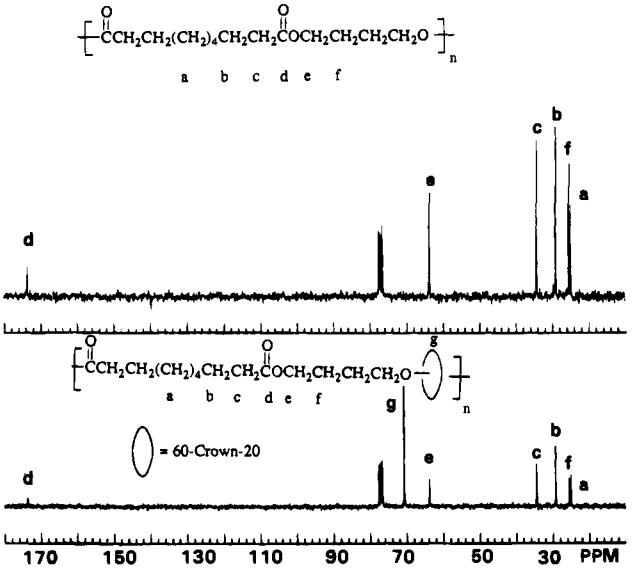

Figure 8. 68 MHz ^{13}C NMR spectra for (a, top) poly(butylene sebacate) (**8a**) and (b, bottom) poly[(butylene sebacate)-rotaxa-(60-crown-20)] (**16**) in $CDCl_3$. The three peaks at δ 77 are due to the solvent.

Ethylene oxide-based crown ethers could also decompose under high temperature and acidic conditions as noted above. A potential product from this decomposition is the oligo(ethylene glycol), which could be incorporated into the polymer through the transesterification reaction. In contrast to the crown ethers **1**−**3**, which display single ^{1}H and ^{13}C NMR resonances,[28] oligo(ethylene glycol)s display multiple resonances. Since polymers **11**−**13** contain triethyleneoxy units, the presence of crown ether-derived oligoethyleneoxy units is not obvious from the NMR spectra, as exemplified by Figures 5 and 6, the ^{1}H and ^{13}C NMR spectra for **7b** and **11b**.

On the other hand, butylene sebacate polymers **14**−**17** afford simpler NMR spectra, so the presence of oligoethyleneoxy units could be detected by ^{1}H and ^{13}C NMR spectroscopy; in fact, no evidence of incorporation of oligo(ethylene glycol)s was observed in **14**−**16**. For example, polyrotaxanes **15** and **16** contain only a single additional peak (for the crown ether component) relative to the model polyester **8a** in ^{1}H and ^{13}C NMR spectra (Figures 7 and 8, respectively). Figure 11 displays the ^{1}H and ^{13}C NMR spectra of the diacetate of poly(ethylene glycol) of $\bar{M}_n$ 600 ($\bar{n}$ = 13.2); note the multiplicity of signals. No such multiple peaks were detected in the ^{1}H and ^{13}C NMR spectra of the polyrotaxanes, clearly confirming the absence of any ethyleneoxy units incorporated into the backbone via ring opening. Also recall that poly(butylene sebacate)

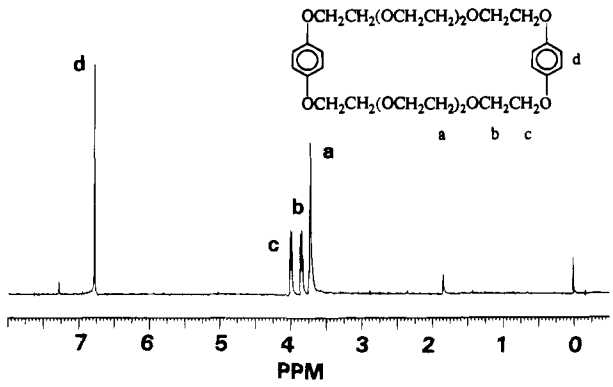

Figure 9. 270 MHz ^{1}H NMR spectrum ($CDCl_3$) of bis(*p*-phenylene)-34-crown-10 (BPP, **4**). The signal at δ 1.85 is due to H_2O complexed with the crown ether. The signal at δ 7.3 is due to $CHCl_3$.

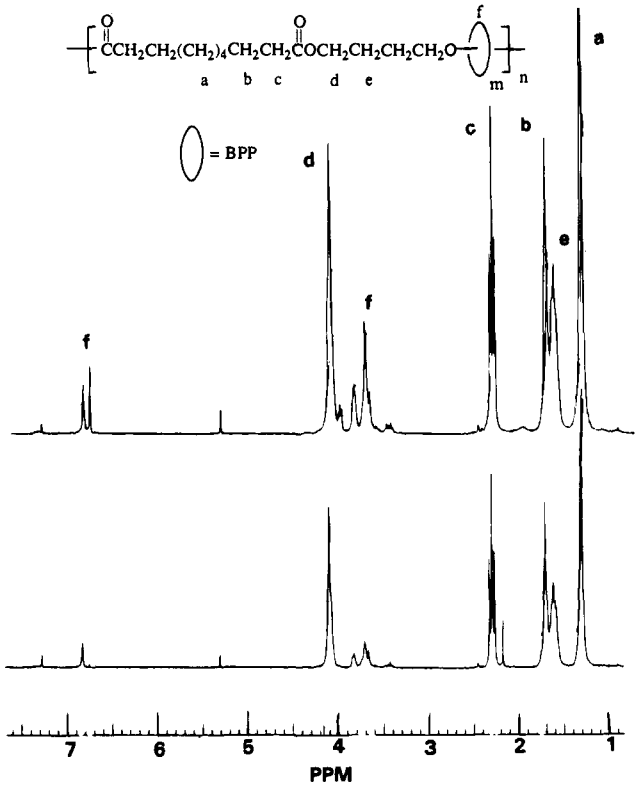

Figure 10. 270 MHz ^{1}H NMR spectra of poly{(butylene sebacate)-rotaxa-[bis(*p*-phenylene)-34-crown-10]} (**17a**) (a, top) after one reprecipitation and (b, botttom) after two reprecipitations. The signal at δ 2.2 (bottom) is due to CH_3COCH_3. The signal at δ 5.3 (top, bottom) is due to CH_2Cl_2. The signal at δ 7.3 (both spectra) is due to $CHCl_3$.

prepared in the presence of 18-crown-6 showed no evidence of ethyleneoxy units by ^{1}H and ^{13}C NMR.

C. Gel Permeation Chromatography and Vapor Phase Osmometry: Polyrotaxane Purity, Molecular Weight, and End-Blocking Efficiency. Most importantly, GPC is capable of detecting the free, unthreaded macrocycle, which has low (<900) molecular weight. Thus GPC confirmed the absence of free 30-crown-10 in poly[(triethyleneoxy sebacate)-rotaxa-(30-crown-10)] (**11b**, sample 144), since only one symmetrical peak was observed (Figure 12b). In contrast, the physical blend of 30-crown-10 (**1**) and poly(triethyleneoxy sebacate) (**7b**) showed two distinct peaks, which correspond to those of 30-crown-10 and the homopolymer **7b**, respectively (Figure 12a). Thus GPC provides a useful method of establishing the purity of polyrotaxanes.

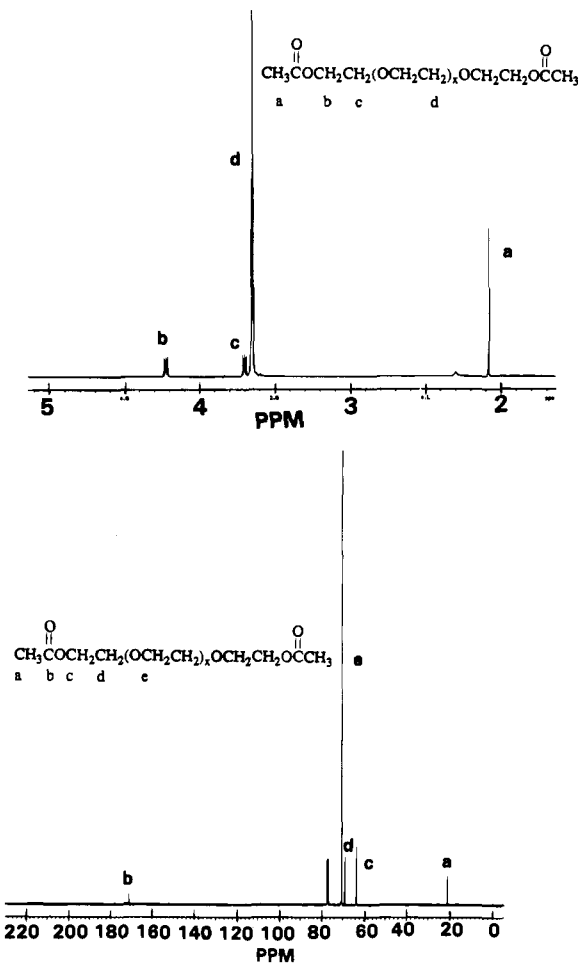

Figure 11. 400 MHz ^{1}H NMR (top) and 101 MHz ^{13}C NMR (bottom) spectra of the diacetate of poly(ethylene glycol), nominal $\bar{M}_n$ = 600 in $CDCl_3$. The three peaks at δ 77 are due to the solvent.

Scheme 3

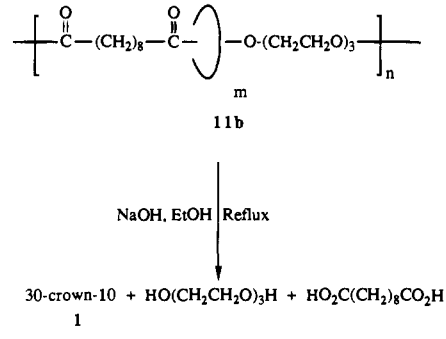

The GPC trace for the mixture of model polymer **7b** and 30-crown-10 (**1**) shown in Figure 12a is interesting in two respects. First, the peak for 30C10 yields on $\bar{M}_n$ value of 450; this is very close to the actual molecular weight of 30C10 (440) and corroborates the universal calibration. Second, the small shoulder at low MW on the main peak may be indicative of some threading of low molecular weight preformed polyester **7b** in solution by 30C10. In later publications, our studies of this process will be discussed.

The molecular weight of polyrotaxane **11b** (sample 144) was determined by both VPO and absolute GPC analyses, and the $\bar{M}_n$ values obtained from these two analyses were 11 000 and 12 000, respectively (Table 4). The molecular weight of polyrotaxane **11b** obtained from VPO reflects the total molecular weight of the polyester backbone and the threaded macrocycle.

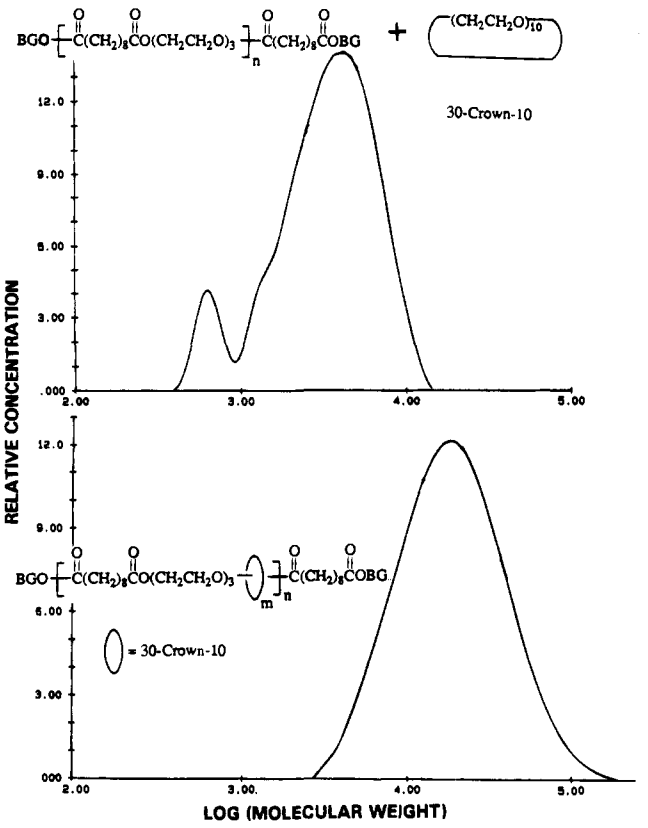

Figure 12. Absolute molecular weight distributions for (a, top) a physical mixture of poly(triethyleneoxy sebacate) (**7b**) (sample 142) and 30-crown-10 (**1**), 95−5 weight percentages and (b, bottom) poly-[(triethylenoxy sebacate)-rotaxa-(30-crown-10)] (**11b**) determined in THF at 30 °C via GPC with viscosity detector and universal calibration. For **11b**, $\bar{M}_n$ = 12.2, $\bar{M}_w$ = 21.6 kg/mol.

When the contribution from 30-crown-10 is subtracted, the $\bar{M}_n$ (~8.4 kg/mol, DP = 26) for the polyester backbone of the polyrotaxane is similar to that ($\bar{M}_n$ = 6.4 kg/mol DP = 20) of the model polyester **7b** produced under similar conditions. This behavior is quite different from that reported for monorotaxanes.[9] In the case of monorotaxanes constructed from a 58-membered crown ether and oligo(ethylene glycol) of $\bar{M}_n$ = 400 ($\bar{n}$ = 8.7) end-capped with trityl groups, the molecular weight obtained from colligative properties was reportedly an average of those of the linear and cyclic components, and the phenomenon has been attributed to the relative freedom of these two components. It is more likely that dethreading, i.e., the reverse process of eq 1, occurred in dilute solution during the VPO experiment with the monorotaxanes, since the triphenylmethyl end-blocking groups were too small to constrain the 30-membered macrocycles, and since the linear species was not polymeric, dethreading occurred rapidly.

The results from our investigation indicate that the macrocycles in polyrotaxane **11b** do not possess such freedom to dethread over periods of a few minutes to several days, and each polyrotaxane molecule behaves like a single particle in solution, as expected. It should be noted in this regard that in **11b** there are six macrocycles per macromolecules on average, or one crown ether per 86 backbone atoms. Indeed, for the sample of **11b** which is represented in Figure 12b (sample 144), dethreading did not occur during GPC analysis; only after 3−10 days in solution was a small amount of dethreading observed (Table 2, sample 3). The absence of dethreading may be due to the chain−macrocycle entanglement in the polyrotaxane, the macrocycles being trapped in random coils of the backbone. If this kind of entanglement does exist, then blocking groups may not be necessary for this polyrotaxane. This speculation is supported by observations from the investigation of polyrotaxanes containing no blocking groups. Polyrotaxane **11a**, prepared similarly to **11b** (sample 3) except that no blocking group was used, showed a similar *n/m* ratio (5.2) after reprecipitations (sample 4, Table 2). No sign of significant dethreading was observed after the first precipitation.

Poly(butylene sebacate) (**8a**), prepared by the transesterification technique in the absence of molecular weight control by the blocking group alcohol, had absolute number average molecular weight ($\bar{M}_n$) of 18.8 kg/mol with polydispersity 1.9 determined by GPC using a viscosity detector (Table 5). The log *K* and *a* values are similar to those for polyester **5a** (Table 1). A GPC trace is shown in Figure 13a for a lower MW sample.

Also shown in Figure 13 are GPC traces for (b) a physical mixture of poly(butylene sebacate) (**8a**) and 42-crown-14 (**2**), (c) 42-crown-14 (**2**) alone, and (d) poly(butylene sebacate)-rotaxa-(42-crown-14)] (**15**), all in chloroform. Note that in the trace b for the physical blend, the presence of the free crown ether is readily detected by the shoulder at larger elution volume. On the other hand, trace d for the polyrotaxane is quite symmetric and shows no evidence of the presence of unthreaded macrocycle. In fact, the polydispersity of the polyrotaxane

Table 4. Molecular Weights (kg/mol) of Model Poly(triethyleneoxy sebacate)s and Corresponding Polyrotaxanes

polymer (sample)	$[n]^a$ (dL/g)	target backbone $\bar{M}_n$	$\bar{M}_n$ ^{1}H NMR	^{13}C NMR	UV[b]	OSM	abs GPC	$\bar{M}_w$ abs GPC	−log *K*	*a*	$\bar{M}_n$ GPC/PS	$\bar{M}_w$ GPC/PS	cyclics per macromolec (av)
7a (SL-139)	0.12	∞					1.9	2.5			2.3	3.9	0
7b (CW-142)		17	7.5[c]			6.4							0
11b (CW-144)		16.8				11.0	12.2	21.6					6.2[d]
11b (CW-3)		16.8											5.2[d]
11c (SL-2-34)	0.28	15.7	9.0[e]		7.5	2.2	2.4	3.6	4.83	1.03	4.4	10.0	2.3[f]
12 (SL-2-25)		∞									3.6	11.6	2.4[g]

[a] In $CHCl_3$ at 30 °C. [b] Using 266 nm absorbance and $\epsilon = 2.88 \times 10^3$ determined for **10** in $CHCl_3$. $\bar{M}_n = 2M(\epsilon)/10(A - 0.037)$, where *M* was the mass of polymer (in mg) dissolved in 10.00 mL of $CHCl_3$ and *A* was the absorbance in a 1.00 cm cell. Estimated experimental error, ±2%. [c] Calculated from $\bar{M}_n = \{(316)(9B)/[A/B) - 2]\} + 2(413) - 132$, where *A* was the integration of the δ 1.3 signal [CH_3 (36H) + $COCC(CH_2)_4CCO$ (8H)] and *B* was that for the δ 1.6 signal [$COCCH_2C_4CH_2CCO$ (4H)]. Estimated error, ±5%. [d] Based on $\bar{M}_n$ = 11.6 kg/mol. [e] Calculated from $\bar{M}_n = \{[316 + 0.31(440)](9B)/[(A/B) - 2]\} + 2(591) - 132 - 0.31(440)$, where *A* was the integration of the δ 1.3 signal [CH_3 (36H) + $COCC(CH_2)_4CCO$ (8H)] and *B* was that for the δ 1.6 signal [$COCCH_2C_4CH_2CCO$ (4H)]. Estimated error, ±5%. [f] Based on $\bar{M}_n$ = 2.3 kg/mol. [g] Based on $\bar{M}_n$ = 3.6 kg/mol.

Table 5. Molecular Weights (kg/mol) of Model Poly(butylene sebacate)s and Corresponding Polyrotaxanes

polymer (sample)	$[n]^a$ (dL/g)	target backbone $\bar{M}_n$	$\bar{M}_n$ ^{1}H NMR	^{13}C NMR	UV[b]	OSM	abs GPC	$\bar{M}_w$ abs GPC	$-\log K$	a	$\bar{M}_n$ GPC/PS	$\bar{M}_w$ GPC/PS	cyclics per macromolec
8a													
(SL-1-145)	0.85	∞				27.6	18.8	35.7	2.66	0.51	19.6	41.7	0
8b													
(SL-1-157)	0.27	5.4	5.2[c] 5.0[d]	5.9[e] 5.4[f]	5.7	5.3					5.0	9.4	0
8b													
(SL-1-169)	0.46	11.4	18.0[c]		18.9	19.3					19.9	33.3	0
15													
(SL-3-42)	0.46	∞									17.0	28.9	15[g]
16													
(SL-1-197)	0.51	∞				8.6	10.1	18.2	3.02	0.54	15.0	24.8	5.9[h]
17b													
(198)		8.8	8.7[i]										1.1[j]

[a] In $CHCl_3$ at 30 °C. [b] Using 266 nm absorbance and $\epsilon = 2.88 \times 10^3$ L/mol cm determined for **10** in $CHCl_3$. $\bar{M}_n = 2M(\epsilon)/10(A - 0.037)$, where M was the mass of polymer (in mg) dissolved in 10.00 mL of $CHCl_3$ and A was the absorbance in a 1.00 cm cell. Estimated experimental error, ±2%. [c] Calculated from $\bar{M}_n = \{256(27)/4[(A/B) - 1\} + 2(592) - 88$, where A was the integration of the δ 1.3 signal [CH_3 (54H) + $COCC(CH_2)_4CCCO$ (8H)] and B was that for the δ 1.5−1.9 signal [$COCCH_2C_4CH_2CCO$ (4H) + $OCCH_2CH_2CO$ (4H)]. Estimated error, ±10%. [d] Calculated from $\bar{M}_n = \{256(27)/2[(A/B) - 2]\} + 2(592) - 88$, where A was the integration of the δ 1.3 signal [CH_3 (54H) + $COCC(CH_2)_4CCCO$ (8H)] and B was that for the δ 2.3 signal [$COCH_2C_6CH_2CO$ (4H)]. Estimated error, ±5%. [e] Calculated from $\bar{M}_n = [256(9)/2(A/B)] + 2(592) - 88$, where A was the integration for the δ 31.37 signal [CH_3 (18C)] and B was that for the δ 29.05 signal ($COCCC_4CCCO$ (4C)). Estimated error, ±5%. [f] Calculated from $\bar{M}_n = [256(3)/(A/B)] + 2(592) - 88$, where A was the integration for the δ 148.2 signal [C_1 arom (6C)] and B was the integration for the δ 173.76 signal [C=O (2C)]. Estimated error, ±7%. [g] Based on $\bar{M}_n = 17.0$ kg/mol. [h] Based on $\bar{M}_n = 9.4$ kg/mol (average of OSM and abs GPC results). [i] Calculated from average of two methods: (1) $\bar{M}_n = \{256(9)/2[(A/B) - 0.667]\} + 2(413)$, where A was the integral for the δ 1.3 signal [CH_3 (54H) + $COCC(CH_2)_4CCCO_2$ (8H)] and B was that for the signals δ 1.5−2.4 [$-OCH_2CH_2CH_2CH_2O-$ (8H) + $COCCH_2C_4CH_2CCO$ (4H)] (9.5 kg/mol); (2) $\bar{M}_n = \{256(26)B/12A\} + 2(413) + 168$, where A was the integral for the signals from δ 7.1−7.4 [arom (8H)] and B was that for the signals δ 1.5−2.4 [$-OCH_2CH_2CH_2CH_2O-$ (8H) + $COCCH_2C_4CH_2CCO$ (4H)] (7.9 kg/mol). Estimated error, ±10%. [j] Based on $\bar{M}_n = 8.7$ kg/mol.

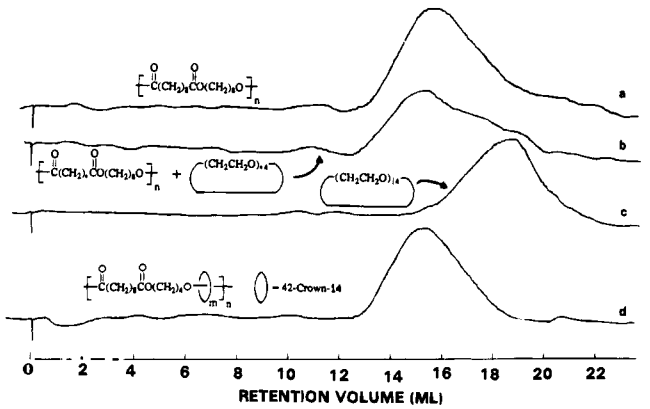

Figure 13. GPC traces for (a) poly(butylene sebacate) (**8a**); (b) a physical mixture of **8a** and 42-crown-14 (**2**) 70:30 by mass; (c) 42-crown-14 (**2**); and (d) poly[(butylene sebacate)-rotaxa-(42-crown-14)] (**15**) in $CHCl_3$ at 30 °C; refractive index detector.

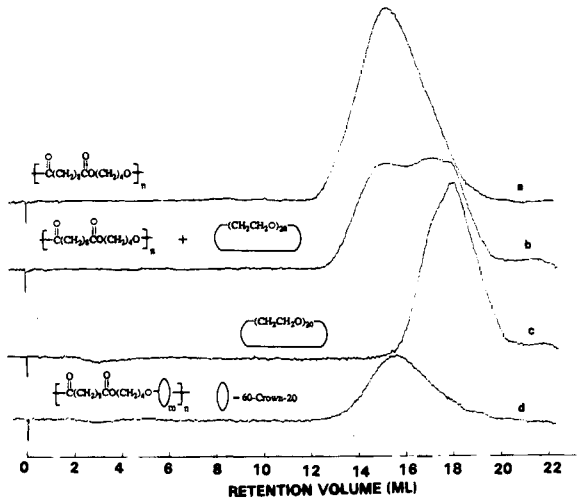

Figure 14. GPC traces for (a) poly(butylene sebacate) (**8a**); (b) a physical mixture of **8a** and 60-crown-20 (**3**), 55:45 by mass; (c) 60-crown-20 (**3**); and (d) poly[(butylene sebacate)-rotaxa-(60-crown-20)] (**16**) in $CHCl_3$ at 30 °C; refractive index detector.

(1.86) is less than that of the polyester model system (2.19). Polyrotaxane **15** was shown by NMR spectroscopy to contain 35 mass % of 42-crown-14, as discussed above.

Similar results for **8a**, a blend of **8a** and 60-crown-20 (**3**), 60-crown-20, and poly[(butylene sebacate)-rotaxa-(60-crown-20)] (**16**) are displayed in Figure 14. Again, although due to the higher molar mass of 60-crown-20, the resolution of the peak for the free macrocycle is somewhat less than with 42-crown-14, on the basis of the symmetry of the peak in curve d relative to that of the blend (curve b), it is evident that polyrotaxane **16** does not contain free crown ether. In fact, the polydispersity of the polyrotaxane, which as shown above contained 51 mass % of 60-crown-20, is less than that of model polyester **8b**, 2.01 vs 2.19 as measured from these traces.

The presence of end-blocking groups allows molecular weights to be estimated by other techniques. Taking advantage of the UV absorption of **10** ($\lambda_{max} = 266$ nm, $\epsilon = 2.88 \times 10^3$), one can calculate $\bar{M}_n$ under the assumption of 100% end-capping. Similarly, the presence of 27 methyl protons in each end-blocking moiety (**10**) enables ^{1}H NMR estimation of $\bar{M}_n$ from integration of the δ 1.3 signal relative to polyester backbone signals, again under the assumption of 100% end-blocking, and knowing the molar ratio of macrocycle to repeat unit. Finally, ^{13}C NMR can be utilized to estimate $\bar{M}_n$ by comparing the integrals for the *tert*-butylmethyl signal (δ 31.37) to that of the four central sebacoyl carbons (δ 29.05) or for the quaternary aromatic carbon (δ 148.2) to the carbonyl carbon (δ 173.76). Polymers end-blocked with **9** were similarly analyzed.

The number average molecular weights of polymers determined by VPO and absolute GPC (universal calibration using viscosity detector) are compared with those determined by other methods in Tables 4 and 5. The end-capping efficiency using **9** or **10** can be calculated by the comparison of number average molecular weight measured by VPO or absolute GPC with that determined by the techniques of end group analysis assuming

two end groups per macromolecule, such as UV spectrometry and ^{1}H NMR.

End-blocked poly(triethyleneoxy sebacate) (**7b**, sample CW-142, Table 4) from NMR analysis had $\bar{M}_n$ = 7900, but osmometry yielded $\bar{M}_n$ = 6400. Thus only 81% end-capping was achieved, i.e., on average only 62% of the macromolecules were blocked at both ends and 38% were blocked at only one end, assuming there are no completely non-end-blocked molecules. For the end-capped poly[(triethyleneoxy sebacate)-rotaxa-(30C10)] (**11c**, sample SL-2-34), M_n values from end group analyses were much higher than the VPO value (Table 4). For example, the UV value was 3.4 times as high as the VPO value, indicating that the end-capping is only 29% complete, i.e., on average there were only 58 blocking groups per 100 molecules.

All the results for poly(butylene sebacate) (**8b**, sample SL-1-157) from different end group techniques are in good agreement with the VPO value (Table 5), indicating the complete end-capping in the case of low molecular weight ($\bar{M}_n$ = 5300). For the higher molecular weight poly(butylene sebacate) (**8b**, sample SL-1-169), however, end-capping also appears to be complete given the larger error inherent in the end group analyses at higher molar masses.

The molecular weights of poly(butylene sebacate)s (**8**) were generally higher than those of poly(triethyleneoxy sebacate)s (**7**) because of formation of THF as discussed before. Since transesterification polymerization was carried out under high vacuum at high temperature and no solvent was used during the reaction, the viscosity of the systems increased at high conversion under these conditions, and magnetic stirring became ineffective at this critical period of polymerization. It is believed that higher molecular weight polymers can be produced by using a mechanical stirrer in larger scale reactions.

For poly(butylene sebacate) (**8a**), there was good agreement between absolute GPC and GPC with polystyrene standards, while VPO yielded a higher value (Table 5). However, end-blocked poly(butylene sebacate) (**8b**) gave good correlation between VPO and GPC with polystyrene standards. For poly-(triethyleneoxy sebacate) (**7a**), absolute GPC and GPC with polystyrene standards also agreed well (Table 4). That is, the hydrodynamic volumes of model polymers **8a**, **8b**, and **7a** are similar to that of polystyrene.

However, for the polyrotaxanes, GPC values with polystyrene standards were always higher than the absolute GPC values and VPO values because of the larger hydrodynamic values of polyrotaxanes relative to polystyrene. For example, poly-[(triethyleneoxy sebacate)-rotaxa-(30-crown-10)] (**11c**) with polystyrene standards yielded an $\bar{M}_n$ value that was twice that of the absolute methods (VPO and absolute GPC) (Table 4), and poly[(butylene sebacate)-rotaxa-(60-crown-20)] (**16**) also yielded a polystyrene equivalent value nearly twice those obtained by absolute methods (Table 5). These results support the idea that rotaxane formation leads to chain stiffening, thereby increasing hydrodynamic volume. The only log K and a values available for comparison (**8a** vs **16**, Table 5), while not showing as large changes as for **5a** and **5b** vs **6** (Table 1), were also indicative of more negative log K and more positive a values for the polyrotaxane. More detailed rationalization of the solution behavior of polyrotaxanes requires more extensive data on the effects of solvents, temperature, etc.

Other experimental results in our laboratory demonstrate a common phenomenon that the molecular weights of step growth polyrotaxanes are often lower than those of the corresponding model polymers. Two factors may be involved: (1) the reaction is retarded by the dilution, solvation, and viscosity effects of the crown ethers and (2) the chain orientations are obstructed or burdened by the threaded macrocycle molecules. Among polyrotaxanes, the poly(butylene sebacate) rotaxanes had much higher molecular weights than the triethyleneoxy analogs. Formation of THF may play a major role in this phenomenon. Strong interactions between the tri(ethylene glycol) molecules and crown ether molecules, both H-bonding and threading, make it difficult to remove excess glycol and drive the equilibrium to high molecular weight polyester.

D. Threading Efficiency of Macrocycles: Effects of Stoichiometry, Ring Size, and Backbone Structure. It has been found that the threading efficiency of the macrocycles is affected by their sizes and their concentrations relative to the monomers.

A higher macrocycle incorporation rate was found in poly-[(triethyleneoxy sebacate)-rotaxa-(60-crown-20)] (**12**) than in poly[(triethyleneoxy sebacate)-rotaxa-(30-crown-10)] (**11a**), and the same phenomenon was observed for poly(butylene sebacate) rotaxanes **14**–**16** with 30-crown-10, 42-crown-14, and 60-crown-20, respectively.

Agam reported that at 1:1 molar ratios of neat components using trideca(ethylene glycol) as the linear component, dibenzo-57-crown-19, a 57-membered ring, leads to 63% threading, while dibenzo-45-crown-15, a 45-membered ring, produces 41% threading.[9] The area of the cavity of the ring is a key variable; it is proportional to the square of the circumference. Thus the cavity area of a fully open 57-membered ring will be 1.60 (57^2/45^2) times as great as that of a 45-membered ring. In this case, the ratio of threading efficiencies (63/41 = 1.54) is very close to this value.

The cavity of a 60-crown-20 molecule is 2 times as large in area as that of a 42-crown-14 molecule and 4 times as large as that of a 30-crown-10 molecule when the macrocycles are fully open. Although the rings are not expected to be fully open in reality and the percentage of threadable conformations is higher for large rings than for small rings,[38] the possibility for a given linear chain to thread should be about 2-fold greater for 60-crown-20 than with 42-crown-14 and 4-fold greater than with 30-crown-10.

For the triethyleneoxy case, even though only half as much 60-crown-20 was used as 30-crown-10 on a molar basis (Table 2, **12**, samples 222 and SL-2-25 vs **11a**, samples 4, 230, and 146), 2.3 times more threading was observed for the larger macrocycle, an overall factor of 4.6 enhancement in threading efficiency. Similarly for the poly(butylene sebacate) rotaxanes, a factor of 4.8 more threading was observed for 60-crown-20 (Table 3, **16**, samples 240 and SL-197) and 2.4 times more efficient threading for 42-crown-14 (**15**, sample SL-3-42) compared to 30-crown-10 (**14**, sample 234).

When the total mass of crown ether in the neat reaction was kept constant in the syntheses of **14** (sample 234), **15** (sample SL-3-42), and **16** (sample SL-197) (Table 3), as shown in Figure 15, the m/n values were proportional to ring size, and the mass percentage of macrocycles in the purified polyrotaxanes also increased linearly with increasing ring size. This phenomenon was also observed in polyurethane rotaxane syntheses.[24] Detailed quantitative analysis of these results is rendered questionable by several factors, including (1) difference in molar concentrations of the crown ethers and (2) the possibility of

(38) This has been demonstrated for cyclic poly(dimethylsiloxane)s using both calculations and experiments. See ref 22.

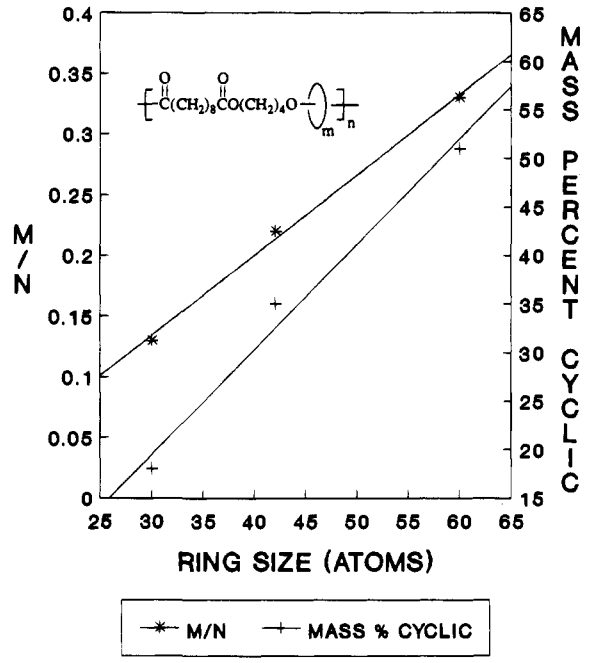

Figure 15. Cyclic ratio (*m/n*) and mass % cyclic in polyrotaxanes **14**, **15**, and **16** as a function of crown ether ring size for neat polymerizations (120 °C, 10 h; 180 °C, 0.1 Torr, 20 h) using the same mass (2.10 g) of each macrocycle per gram of dimethyl sebacate.

loss of macrocycles from the non-end-capped polyrotaxanes by dethreading during purification, particularly in the first precipitation.[39]

In the case of **16**, as expected on the basis of the equilibrium nature of the threading process depicted in eq 1, variation of the molar feed ratio of dimethyl sebacate to 60-crown-20 from 3.17 (sample 232, Table 3) to 1.86 (samples 240 and SL-197) caused a substantial increase in macrocycle content from 44 to 50 mass %. Similar results were obtained with polyurethane rotaxanes.[24]

In the case of BPP-based polyrotaxane **17**, inclusion of a blocking group (**17b**, sample 198, Table 3) resulted in no essential change in macrocycle content relative to the non-end-blocked system **17a** (sample 196), as also was observed with **11a** vs **11b** (samples 4 and 3, Table 2), perhaps also due to incomplete end-blocking, whose efficiency was not determined in this case.

The importance of interactions of the macrocycle with the backbone was probed by comparison of the threading efficiencies of the triethyleneoxy and butylene systems with 30-crown-10 (Table 2, **11a**, samples 4, 230, and 146 vs Table 3, **14**, sample 234). For the same feed ratio, the triethyleneoxy polymer **11a** contained one macrocycle per 5.2 repeat units, as compared to one per 7.8 in the butylene system **14**. On a backbone atom basis (20 per repeat unit in **11a** vs 16 in **14**), the triethylenoxy polymer had an average one 30-crown-10 per 107 atoms, while the butylene polymer had one per 125 atoms; in other words, the triethyleneoxy threading efficiency was 17% higher on this basis. Probably two factors are involved: (1) the longer triethylene glycol (10 atoms in its backbone) may achieve a higher number of threadings than the shorter (six atoms) butylene glycol (as shown for other systems[7-10] and (2) the greater compatibility of the triethyleneoxy moiety with the crown ether may contribute as well. The effect of the length

(39) Indeed, based on recent experiments, we believe that with the present systems a fraction of the threaded macrocycles is lost in the first precipitation by dethreading. Hence, the threading efficiencies reported here should be viewed as minimal.

Table 6. Solubility of Polysebacates and Polysebacate Rotaxanes

polymer (sample)	water	methanol	acetone (hot)	CH_2Cl_2	THF
7a (SL-1-139)	no	no	no	yes	yes
8a (SL-1-145)	no	no	no	yes	yes
11b (3)	slightly	slightly	yes	yes	yes
11c (SL-2-34)	slightly	slightly	yes	yes	yes
12 (SL-2-25)	slightly	slightly	yes	yes	yes
15 (SL-3-42)	slightly	slightly	partially	yes	yes
16 (SL-1-197)	slightly	slightly	yes	yes	yes

of the monomer and corresponding ester oligomers on the threading efficiency is probably greater than that of the compatibility of macrocycles and polymer backbones. Experiments on the poly(tetramethylene oxide) and polybutadiene rotaxanes showed that the nature of the backbone in terms of compatibility was not as important as its length.[26]

BPP (**4**), because of the open cavity ("molecular box") shown in is X-ray crystal structure[13b] brought about by the rigid phenylene units and the short ethyleneoxy tethers, was expected to be ideal for statistical rotaxane formation. As shown in Tables 2 and 3, however, this is not the case; only small amounts (≤6 mass %) of threaded BPP were incorporated into the polysebacates **13** and **17**, either with or without end-blocking groups [samples 212 (**13**), Table 2, and 196 (**17a**) and 198 (**17b**), Table 3]. We might attribute the low cyclic content of **13** to the fact that a 4-fold lower feed ratio was used compared to the 30C10 system **11a**. When this is considered, the threading efficiencies of BPP and 30C10 are more comparable. However, the cyclic/monomer ratios for **17a** and **17b** were comparable to those for **14**, and the threading efficiency of BPP was much lower than 30C10. Our explanation is that in the melt at elevated temperatures, the cavity of BPP is in fact not open but instead is effectively closed by rapid rotation of the *p*-phenylene rings, a process we call the "saloon door mechanism". This result provides a note of caution in extrapolation of solid state structures to the solution phase.

Finally, it is of interest to compare the transesterification polymerization methodology to the diacid chloride–diol technique. This can be done in a crude way by comparing 30-crown-10-based systems **14** (Table 3) and **6** (Table 1). **14** has a butylene sebacate backbone, while **6** has a decamethylene sebacate repeat unit, and 3 times more crown ether was used in synthesis of **6** than **14**. The *m/n* ratios were 6.7 for **6** and 7.8 for **14**, 16 vs 18 mass % cyclics, respectively. Taking into account the differences, including temperatures, these are comparable values. In other words, the two approaches yield similar levels of macrocycle incorporation into the polyrotaxanes.

E. Solubility Properties of Polyrotaxanes. As shown in Table 6, all of the polyrotaxanes displayed solubility behavior that differed from that of the simple linear polyesters themselves. The former display higher solubility in polar solvents than the latter. This was also observed with polyurethane rotaxanes[24] and most strikingly with poly[(acrylonitrile)-rotaxa-(60-crown-20)], which is completely soluble in methanol.[25]

Poly(triethyleneoxy sebacate) rotaxanes **11–13** are substantially more soluble in polar solvents than the parent polyester **7a**. For example, **11b**, *n/m* = 5.1 (sample 3), in spite of its hydrophobic blocking groups, is somewhat soluble in methanol

and acetone, while poly(triethyleneoxy sebacate) (**7a**) is completely insoluble in methanol and acetone.

Likewise, the rotaxanes based on poly(butylene sebacate) reflect the enhanced polar contribution of the macrocycles. For example, while the parent polyester **8a** is virtually insoluble in methanol and acetone and is isolated in 96% yield after two precipitations from methanol, polyrotaxane **16**, n/m = 3.3 (sample SL-197), is slightly soluble in methanol and completely soluble in acetone, affording only a 32% yield after two precipitations from methanol. Even with the use of water as a precipitation medium, only 30% of the polymer was recovered after three reprecipitations!

Just as in covalently bonded copolymers, the solubility properties of polyrotaxanes should reflect the properties of the two components. Thus the solubility parameter of a polyrotaxane should be a function of its composition, as well as the size and flexibility of the macrocycles. Enhancement of solubilities of polyrotaxanes in polar solvents increases with increasing crown ether content; for example, polyrotaxane **15** is only partially soluble in acetone because of its lower crown ether content compared to polyrotaxane **16**, which is completely soluble in acetone. However, because of the mobility of the cyclic species along the linear backbone, some unusual behavior may be anticipated. For example, good solvents for the backbone which are poor solvents for the macrocycle may lead to aggregation and crystallization of the cyclic component. Conversely, good solvents for the macrocycle that are poor solvents for the backbone may force backbone segments that are not in the vicinity of the cyclic species to remain in a highly coiled state. To date we have not explored these possibilities, but we plan to do so because they should significantly affect solution properties such as radius of gyration, hydrodynamic volume and dethreading, and micelle formation,[40] as well as crystallization of the cyclics.

F. Thermal Transitions and Bulk Properties of Polyrotaxanes. All of the polyrotaxanes exhibited phase transition behavior that differed from that of the simple corresponding model polyester. Both glass transitions and melting points were altered, and in some cases the macrocycles were able to crystallize without dethreading.

1. Poly(triethyleneoxy sebacate) Systems. The model system poly(triethyleneoxy sebacate) (**7a**) displayed complex phase transition behavior, as shown in Figure 16. Upon heating (Figure 16a), a glass transition occurred at −56 °C, immediately followed by a crystallization exotherm at −47 °C, and then a melting endotherm at −26 °C, another crystallization exotherm at −23 °C, a broad double-peaked melting transition at 19 °C, a small endothermic transition at 30 °C, and finally a melting transition at 36 °C. The second run after slow cooling (Figure 16b) essentially reproduced the first heating, except that the two uppermost endothermic transitions were absent. These two transitions reappear only after several days of "annealing" at room temperature. Essentially the same results were observed for the end-blocked analog **7b** (not shown), except that the two highest temperature endothermic events were never observed. The nature of the complex set of transitions was not further investigated, since our intent was to use the parent system as a point of reference for the corresponding polyrotaxane derivatives. In the only report we found on this system, T_m was reported to be 28 °C.[33]

(40) Indeed, rotaxanes based on crown ethers and polyurethanes are soluble in water at room temperature and display lower critical solution temperatures at 80 °C. Micelles have been detected by light scattering [unpublished results of R. Davis, Y. X. Shen, and H. W. Gibson]. Poly[(styrene)-rotaxa-(crown ether)]s form emulsions in water and alcohols [unpublished results of S.-H. Lee and H. W. Gibson].

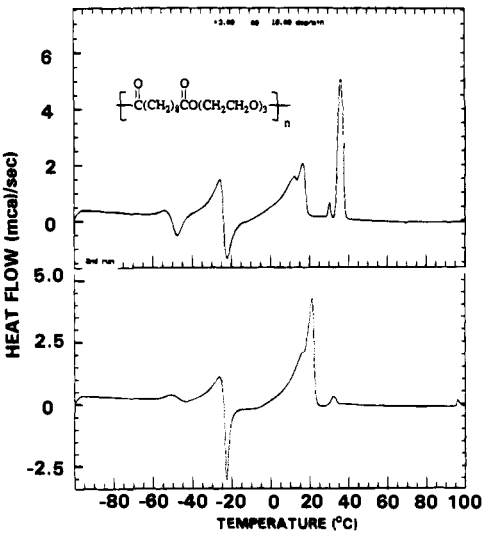

Figure 16. DSC traces for poly(triethyleneoxy sebacate) (**7a**, sample SL-139): (a, top) first heating scan and (b, bottom) second heating scan after slow cooling, 10 °C/min. Temperature scale is uncorrected.

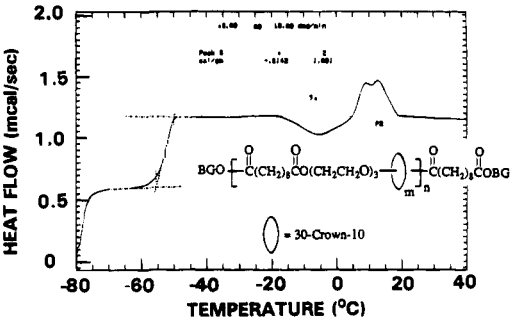

Figure 17. DSC trace for poly[(triethyleneoxy sebacate)-rotaxa-(30-crown-10)] (**11c**, sample SL-2-34), 10 °C/min. Temperature scale is uncorrected.

The DSC trace for the heating of the end-blocked triethyleneoxy sebacate polyrotaxane based on 30-crown-10 (**11c**) is shown in Figure 17. The glass transition is clearly obvious at −56 °C. Similarly to that for the model polyester **7a** (Figure 16), a cryatallization exotherm was observed at −8 °C, followed by a double-peaked endotherm at 10 °C. Upon cooling of the sample at 5 °C/min to −40 °C, no transitions were observed. Subsequent heating curves reproduced the first heating curve. Thus, in this case, rotaxane formation did not significantly alter the phase behavior of the polyester.

However, in the 60-crown-20-based system **12**, whose DSC curves are shown in Figure 18, a new phenomenon was observed. Upon heating (Figure 18a), in addition to the glass transition temperature at −57 °C, a small melting endotherm occurred at 12 °C, and then a large melting transition occurred at 43 °C. Upon cooling of the sample at 10 °C/min (Figure 18b), a single large crystallization exotherm was seen at 13 °C. After rapid cooling to −100 °C, heating produced a crystallization exotherm at −45 °C and the subsequent melting transition at 43 °C. Figure 19 illustrates the phase transition behavior of 60-crown-20 (**3**), which underwent melting at 56 °C (Figure 19a) and upon slow cooling crystallized at 36 °C (Figure 19b); after rapid cooling the glass transition was observed at −67 °C. In view of the fact that poly(triethyleneoxy sebacate) (**7a**) itself displayed no endothermic transitions above 36 °C and did not readily re-form this crystalline phase upon cooling (Figure 16), the crystalline phase in polyrotaxane **12** is attributed to the crown ether. The transition temperatures observed in polyrotaxane **12** were somewhat depressed relative

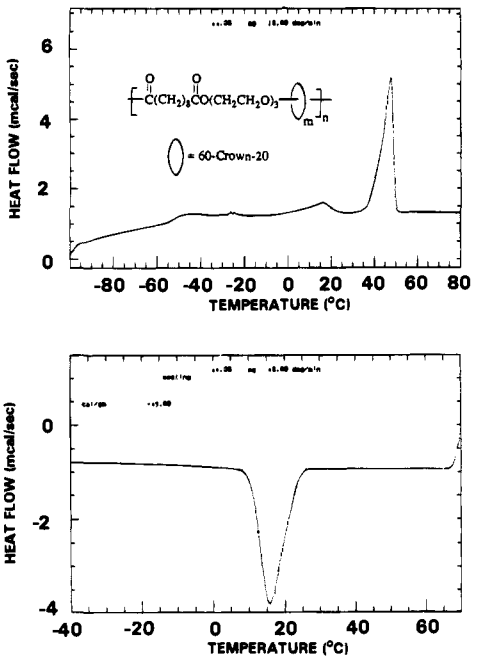

Figure 18. DSC traces for poly[(triethyleneoxy sebacate)-rotaxa-(60-crown-20)] (**12**): (a, top) heating and (b, bottom) cooling, 10 °C/min. Temperature scale is uncorrected.

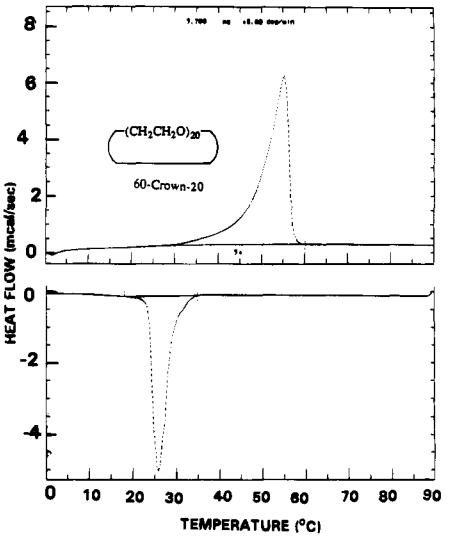

Figure 19. DSC traces for 60-crown-20 (**3**): (a, top heating, 10 °C/min; (b, bottom cooling, 5 °C/min. Temperature scale is uncorrected.

to the pure macrocycle **3**, as would be expected. The perfection of the crystal of the macrocyclic component of the polyrotaxane should be lower than that of the macrocycle itself due to the constraints of the linear backbone penetrating the crown ether; the aggregation of the cyclic species required for recrystallization will likewise be retarded by the physical linkage. Such crystallization of the cyclic component of polyrotaxanes was observed with amorphous polyurethane backbones as well.[24]

2. Poly(butylene sebacate) Systems. Poly(butylene sebacate) (**8a**) is a highly crystalline polymer, T_m = 64−67 °C, and T_g was not observed by DSC (Table 7); the heating and cooling curves (DSC) are shown in Figure 20. T_m of **8a** has been reported as 63−65 °C and T_g as −57 to −75 °C.[35,36,41] End-capped poly(butylene sebacate) **8b** shows a somewhat lower T_m, dependent of course on molecular weight; compare **8a** (samples SL-1-145 and CW-175) and **8b** (samples SL-1-157 and SL-1-169) in Table 7.

However, poly[(butylene sebacate)-rotaxa-(42-crown-14)] (**15**, sample SL-3-42), as shown in Table 7 and Figure 21a, displayed a T_g at −58 °C and *two* melting transitions, one at 53 °C and the other at 59 °C. Upon cooling, crystallization exotherms occurred at 48 and 16 °C (Figure 21b). The melting point of pure 42-crown-14 was 56 °C, as shown in Figure 22a. Upon cooling from the melt, it crystallized at 32 °C (Figure 22b). Its T_g was −68 °C.[28]

Thus, it appears that for polyrotaxane **15**, T_g corresponds to that of the crown ether and that the two melting and crystallization transitions are associated with crown ether and backbone-rich domains. That is, the sharper transitions at higher temperature on heating and cooling (Figure 21) are due to backbone transitions, and the smaller lower temperature events are due to the crown ether. The polyester melting and crystallization transitions are sharper and closer to those of the pure component than those of the crown ether, indicating that the backbone crystallization process is less influenced by rotaxane formation than the crystallization of the crown ether. Hence, the lamellar perfection of the polyester is greater than the ordering of the crown regions of the polyrotaxane. Taking into account the fact that the sample was 35 mass % macrocycle, comparison of the heats of crystallization from Figures 21b, 20b, and 22b indicate that ~80% of the backbone and ~14% of the macrocycle species of **15** crystallized with respect to the pure components **3** and **8a**.

Moreover, polyrotaxane **16** showed a T_g at −60.5−56 °C (Table 7) in the vicinity of the glass transition temperature of 60-crown-20 itself (−67 °C). Two melting points were observed for polyrotaxane **16** (sample CW-178, Figure 23a) at

Table 7. Thermal Properties of Model Polymers and Polyrotaxanes

polymer (sample)	TGA[a] (°C, 5% loss)	T_g[b] (°C)	T_m[b] (°C)	ΔH_f (cal/g)	T_c,[c] heating (°C)	T_c,[d] cooling (°C)
7a (SL-1-139)	273	−55.5	−26, 19[e] 30, 36	7.4, 15.3	−47, −23	−0.6
7b (CW-142)	313	−63	−39, 9		−50, −24	−16
8a (SL-1-145)	340		67[f]	18.5[f]		48
8a (CW-175)	384		64[f]	14.4[f]		
8b (SL-1-157)	312		62	14.7		40.7
8b (SL-1-169)	320		65	20.1		
11b (CW-144)		−54	5, 18		−9	
11c (SL-2-34)	222	−55.7	9, 13	1.06 tot[e]	−8	
12 (SL-2-25)	277	−56.9	43	11.6	−44	15
15 (SL-3-42)	258	−58	53, 59	5.1, 16.0		48, 16
16 (SL-1-197)	298	−60.5	33, 37	15.5 tot[e]	−49	19, 9
16 (CW-178)	288	−55.6	48, 59[b]			

[a] Measured in air at 10 °C/min. [b] At 10 °C/min after heating to melt and cooling to −100 °C; corrected. [c] At 10 °C/min after rapid cooling from the melt; corrected. [d] At 2.5 °C/min; corrected. [e] Broad peak; two maxima. [f] Reported T_m values are 62.6,[34] 64.8,[35], and 64.5 °C;[40] ΔH_m = 37.0 cal/g for sample of $\bar{M}_v$ = 2.5 kg/mol.[35]

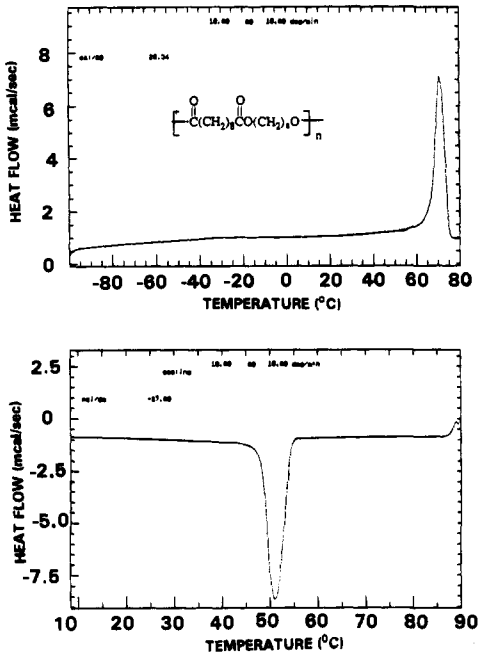

Figure 20. DSC traces for poly(butylene sebacate) (**8a**, sample SL-1-145): (a, top) heating and (b, bottom) cooling, 10 °C/min. Temperature scale is uncorrected.

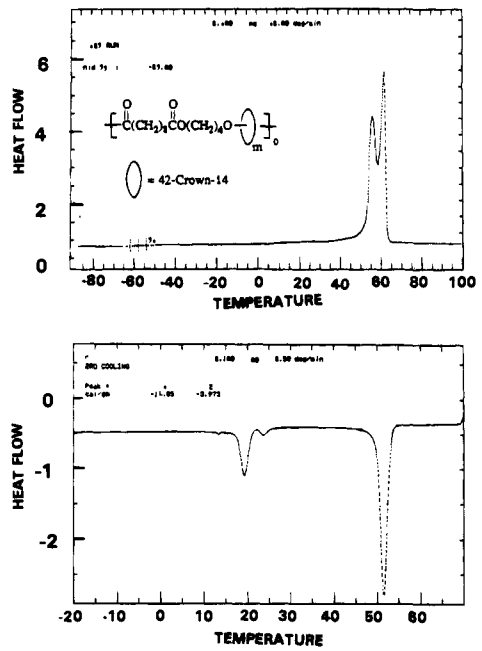

Figure 21. DSC (a, top) heating (10 °C/min) and (b, bottom) cooling (2.5 °C/min) traces for poly[(butylene sebacate)-rotaxa-(42-crown-14)] (**15**). Temperature scale is uncorrected.

48 and 59 °C, slightly below the melting points of 60-crown-20 (**3**) (57 °C, Figure 19) and polymer **8a**, (66 °C, Figure 20), respectively. This behavior is similar to that of block copolymers, which are often heterogeneous on a microscopic scale. Phase separation might take place via dethreading. However, our tests shows that no dethreading occurs at room temperature in solution, and this conclusion was corroborated for the melt state by the reproducibility of the DSC results and by the results described below.

Physical blends of 60-crown-20 (**3**) and poly(butylene sebacate) (**8a**) were also examined by DSC analyses (Figure 23b). Two melting points, much closer to those of the individual pure components, and two crystallization temperatures were observed

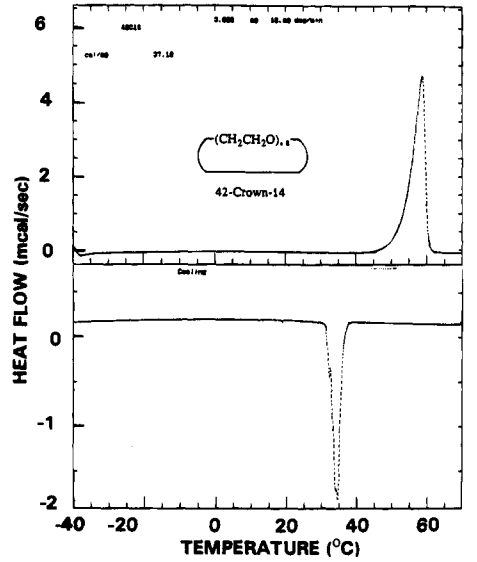

Figure 22. DSC traces for 42-crown-14 (**2**): (a, top) heating and (b, bottom) cooling, 10 °C/min. Temperature scale is uncorrected.

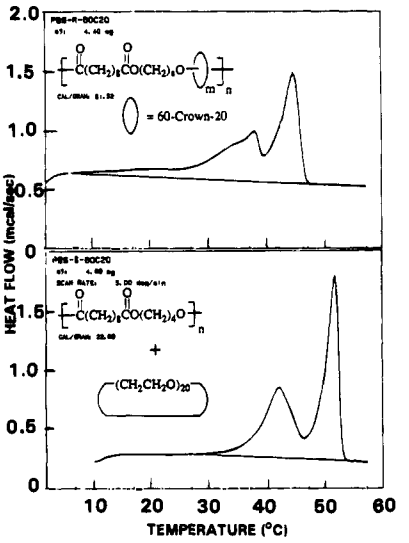

Figure 23. DSC heating (5 °C/min) traces for (a, top) poly[(butylene sebacate)rotaxa-(60-crown-20)] (**16**) and (b, bottom) a physical mixture of poly(butylene sebacate) (**8a**) and 60-crown-20 (**2**) with the same 60-crown-20 contents (50 wt %). Temperature scale is uncorrected.

for the blend material, since 60-crown-20 and poly(butylene sebacate) have distinctly different melting and crystallization behaviors and they are not compatible with each other. Similar to other incompatible binary blends, there are two crystalline phases, therefore, corresponding to 60-crown-20 and polysebacate, respectively.

Poly[(butylene sebacate)-rotaxa-(60-crown-20)] (**16**) and its topological counterpart, the physical blend of poly(butylene sebacate) (**8a**) and 60-crown-20 (**3**) with the same chemical composition, were also examined using optical microscopy.[42] These two materials had very different morphologies. The polyester rotaxane was a homogeneous material which melted completely at 65 °C. Upon cooling, spherulites formed and grew uniformly throughout the entire mass, and the crystallization process was completed in 15 min at 46 °C. On the other hand, the physical blend was grossly heterogeneous, and a higher temperature was required for the system to melt completely. Upon cooling, spherulites first formed and grew slowly in the polysebacate regions. After the crystallization was complete

(41) Marvel, C. S.; Johnson, J. H. *J. Am. Chem. Soc.* **1950**, *72*, 1674.

in all polysebacate domains and the temperature was lowered to 35 °C, spherulites started forming and growing in the crown ether domains. The growth rate of the polyester crystallites in the rotaxane was more than 10 times slower than that in the blend or pure polyester.[42]

The fact that polyrotaxanes **15** and **16** possessed two melting points and two crystallization temperatures is quite interesting, especially when coupled to the similar results for polyrotaxane **12**. Two deductions can be made. (1) Since there are two kinds of crystalline phases in these systems, there must be enough freedom for the macrocycles to move along the polymer backbone during the crystallization process so that both the macrocycle and the polymer backbone can aggregate and crystallize independently. (2) The significant depression in both the melting points and the crystallization temperatures and the lower degree of crystallization as indicated by lower heats of fusion for the polyrotaxanes relative to the pure linear and cyclic components indicate that the crystallization process, however, is hindered by the "permanent" physical linkages between macrocycles and linear polymer chains in the polyester rotaxanes.[42] Detailed study and discussion of these processes will be reported separately.

G. Thermooxidative Stability of Polyrotaxanes. Because crown ethers are not thermally stable in air, polyrotaxanes tend to decompose at lower temperatures compared to their linear analogs, as shown by the TGA results in Table 7.

Conclusions

We have demonstrated here that polymeric rotaxanes can be synthesized by polyesterification using macrocycles as solvents in both diacid chloride−diol and transesterification methods. Significant amounts, up to 55 mass %, of the macrocyclic component can be incorporated. The threading of macrocycles onto the backbone leads to changes in physical properties, including solubility and glass transition temperature. Due to the ability of the macrocycles to move along the backbone and aggregate, the macrocycles are able to crystallize without dethreading.

Experimental Section

General. All melting points were determined on a Haake-Buchler melting point apparatus and are corrected. ^{1}H NMR spectra were recorded with chloroform solutions (unless otherwise noted) on a Bruker 270 MHz instrument and a Hewlett Packard 7550A graphics plotter or a Varian Unity 400-MHz instrument. ^{13}C NMR spectra were recorded on chloroform solutions (unless otherwise noted) using Bruker WP-200, Bruker WP-270, or Varian Unity 400 MHz instruments; chemical shifts are relative to the center line of the $CDCl_3$ triplet at 77.0 ppm. Fourier transform infrared (FTIR) (KBr pellets unless otherwise noted) spectra were recorded on a Nicolet MX-1. Elemental analyses were performed by Atlantic Microlab (Norcross, Georgia). Thermogravimetric analyses (TGAC) were carried out on a DuPont 951 TGA coupled to a DuPont instruments Thermal Analyst 2100. Transition temperatures (T_g, T_m) were determined by a dual cell DuPont Instruments 912 differential scanning calorimeter (DSC) coupled to the same data station as in TGA or a Perkin-Elmer DSC 2 at a heating rate of 10 °C/min or less. Absolute molecular weights were determined from gel permeation chromatography (GPC) analyses run on a Waters 150C equipped with a refractive index detector and Viscotek Model 100 differential viscosity detector using the universal calibration approach which relates elution volume to the product $[\eta][M]$. GPC measurements were also done using a Waters 590 instrument fitted with refractive index and UV detectors which was calibrated with polystyrene standards. Permagel 10^2-10^6 Å polystyrene−divinylbenzene columns were employed in both instruments. VPO data were recorded on a Wescan-232A molecular weight apparatus at 63 °C using toluene as solvent, and the molecular weights were calculated using a calibration curve obtained from squalane (MW 411), sucrose octaacetate (MW 678), and polystyrene (MW 1250, 2150, 2950, 5050, 9200, and 22 000). Ultraviolet spectra were obtained on a Perkin-Elmer Model 330 instrument. Intrinsic viscosities were measured on polymer solutions by the successive dilution technique beginning with a 1% by weight solution of the polymer in a Cannon-Fenske type viscometer; care was taken to have the measured t (flow time, solution) values between 1.7 and 1.1 t_0 (flow time, solvent).

30-Crown-10 (1), 42-Crown-24 (2), and 60-Crown-20 (3). 30-Crown-10 and 60-crown-20 were synthesized[28,29] from hexa(ethylene glycol) and tetra(ethylene glycol) ditosylate using NaH as base. They were separated and purified by fractional crystallization. Pure 30-crown-10 (25% yield) had T_m = 43.8 °C (DSC, 2.5 deg/min); lit.[43] mp 33.5−38.0 °C, oil;[44] ^{1}H NMR (δ) 3.67 (s); ^{13}C NMR δ 70.7; and MS 441 (M + 1, CI), 149, 89. Pure 60-crown-20 (48% yield) had T_m = 57.2 °C, T_g = −67 °C (after quenching from the melt) (DSC, 2.5 deg/min); lit.[44] mp 46−50.5 °C; ^{1}H NMR δ 3.64 (s); ^{13}C NMR δ 70.5; and MS 882 (M + 1) 89, 177. 42-Crown-14 was made from tetra(ethylene glycol) and tri(ethylene glycol) ditosylate (52% yield):[28] T_m = 56 °C (DSC, 10 deg/min); lit.[45] mp 28.5−31.0 °C; ^{1}H NMR δ 3.64 (s); and MS 617 (M + 1, CI), 177, 133.

Bis(*p*-phenylene)-34-Crown-10 (3). This macrocycle was prepared from hydroquinone and tetra(ethylene glycol) ditosylate via either the single-step method[46] or the four-step procedure.[13a] Pure BPP had mp 94.3−95.6 °C; lit.[46] mp 93.5−94.0 °C, lit.[13a] mp 87.0−89.0 °C; ^{1}H NMR δ 3.70 (m, 16H), 3.80 (m, 8H), 4.00 (m, 8H), 6.80 (s, 8H); and ^{13}C NMR δ 68.12, 69.77, 70.70, 70.80, 115.50, 153.05.

3,3,3-Triphenylpropionyl Chloride. 3,3,3-Triphenylpropionic acid (5.04 g, 16.7 mmol) was refluxed for 7 h in $SOCl_2$ (32.6 g, 0.27 mol). The excess $SOCl_2$ was evaporated, and the solid was recrystallized from ethyl acetate/hexane. When the crystals were filtered and dried under vacuum for 5 h, 3.09 g (58%) of pure material was obtained: mp 120.0−123.0 °C, lit.[47] mp 127−128 °C; IR (cm^{-1}) 1807 (C=O), 1492, 1444, 1392; and ^{1}H NMR δ 4.40 (s, 2H), 7.10−7.40 (m, 15H).

Methyl 3,3,3-Triphenylpropionate. 3,3,3-Triphenylpropionic acid (1.50 g, 4.96 mmol) was dissolved in a mixture of 5 mL of methanol and 20 mL of 2,2-dimethoxypropane. To this was added 1.0 mL of concentrated HCl, and stirring was continued overnight. The mixture was poured into 10% HCl and extracted three times with CH_2Cl_2, which was dried over $MgSO_4$ and evaporated to give a yellow solid. Recrystallization from ethyl acetate/hexane gave 1.07 g (69%) of solid with mp 124.5−125.2 °C. A second recrystallization yielded 1.00 g of a slightly yellow solid: mp 124.5−125.2 °C; lit.[48] mp 120.0−121.5 °C; NMR δ 3.40 (s, 3H), 3.70 (s, 2H), 7.2 (m, 15H); UV ϵ = 774 at 260 nm (THF) from a Beer's law plot over a concentration range that afforded absorbances between 0.15 and 0.9.

Poly(decamethylene sebacate), Not End-capped (5a) (Sample 157, Table 1). Recrystallized 1,10-decanediol (0.8268 g, 4.74 mmol) was dissolved in 10 mL of dry diglyme and brought to 90 °C, and distilled sebacoyl chloride (1.00 mL, 1.12 g, 4.69 mmol) was added. The polymerization was continued at 90−100 °C for 43 h. The solution was cooled to 25 °C; the solid mixture was dissolved in a minimal amount of $CHCl_3$ and precipitated into 700 mL of methanol. The solid was filtered and dried under vacuum overnight, and 1.4445 g (90%) of polymer was obtained: IR (cm^{-1}) 1734 (C=O), 1175; ^{1}H NMR δ 1.32 (m, 20H), 1.64 (t, J = 7 Hz, 8H), 2.30 (t, J = 8 Hz, 4H), 4.05 (t, J = 8 Hz, 4H).

Poly(decamethylene sebacate), End-capped (5b) (Sample 161, Table 1). Recrystallized 1,10-decanediol (0.8242 g, 4.73 mmol) was dissolved in 10 mL of dry diglyme and brought to 90 °C, and distilled sebacoyl chloride (1.00 mL, 1.12 g, 4.69 mmol) was added. The polymerization was continued at 90 °C for 43 h. To this was added 3,3,3-triphenylpropionyl chloride (0.32 g, 1.00 mmol), and the reaction

(42) Marand, H.; Prasad, A.; Wu, C.; Bheda, M.; Gibson, H. W. *Am. Chem. Soc. Div. Polym. Chem., Polym. Prepr.* **1991**, *32* (3), 639.
(43) Vitali, C. A.; Masci, B. *Tetrahedron* **1989**, *45*, 2201.
(44) Deslongchamps, P.; Lamothe, S.; Lin, H. S. *Can. J. Chem.* **1987**, *65*, 1298.
(45) Chenevert, R.; D'Astous, L. *J. Heterocycl. Chem.* **1986**, *23*, 1785.
(46) Helgeson, R. C.; Tarnowski, T. L.; Timko, J. M.; Cram, D. J. *J. Am. Chem. Soc.* **1977**, *99*, 6411.
(47) Wittig, G.; Schloder, H. *Justus Liebigs Ann. Chem.* **1955**, *592*, 38.
(48) McElvain, S. M.; Morris, L. R. *J. Am. Chem. Soc.* **1952**, *74*, 2657.

was continued for 4 h. The polymer was isolated as described above, for 1.4938 g (94%) of end-capped polyester: IR (cm^{-1}) 1734 (C=O), 1175; ^1H NMR δ 1.32 (m, 20H), 1.64 (t, J = 7 Hz, 8H), 2.30 (t, J = 8 Hz, 4H), 3.72 (s, 0.1H, $(C_6H_5)_3CCH_2$), 4.05 (t, J = 8 Hz, 4H), 7.26 [s, 0.8H $(C_6H_5)_3C$]; UV, A = 0.428 in a 1 cm cell for a solution of 29.57 mg in 10 mL of THF and A = 0.634 in a 1 cm cell for 42.74 mg in 10 mL of THF; calcd $\bar{M}_n$ = 10.7 kg/mol assuming 100% end-capping.

Poly[(decamethylene sebacate)-rotaxa-(30-crown-10)] (6) (Sample 177, Table 1). Recrystallized 1,10-decanediol (0.8262 g, 4.741 mmol) was suspended in 30-crown-10 (7.1630 g, 16.2 mmol) and stirred at 90 °C for 2 h; the mixture became homogeneous. Sebacoyl chloride (1.00 mL, 1.12 g, 4.69 mmol) was added, and the polymerization was continued for 40 h. 3,3,3-Triphenylpropionyl chloride (0.32 g, 1.00 mmol) was added, and the reaction mixture was stirred for an additional 4 h. The solution was cooled, and $CHCl_3$ was added before it solidified. The polymer was precipitated in 700 mL of ethanol and filtered. The ethanol was evaporated, and macrocycle was recovered: ^1H NMR (first precipate) 1.32 (s, 20H), 1.64 (t, J = 7 Hz, 8H), 2.30 (t, J = 8 Hz, 4H), 4.10 (t, J = 8 Hz, 4H), 3.67 (s, 9.25H), 7.26 (s, 1.2H) (the signal at δ 3.67 is due to 30-crown-10); UV (first precipitate), A = 0.530 in a 1 cm cell for a solution of 18.53 mg in 10 mL of THF; calcd $\bar{M}_n$ = 5.5 kg/mol assuming 100% end-capping; UV (second precipiate), A = 0.981 in a 1 cm cell for a solution of 37.58 mg in 10 mL of THF; calcd $\bar{M}_n$ = 6.0 kg/mol; UV (third precipitate), A = 0.542 in a 1 cm cell for a solution of 20.76 mg in 10 mL of THF; calcd $\bar{M}_n$ = 6.0 kg/mol.

Poly(triethyleneoxy sebacate) (7a) (Sample SL-139) (General Procedure). Stage 1. To a 15 mL flask were added dimethyl sebacate (DMS) (1.83 g, 7.96 mmol), tri(ethylene glycol) (TEG) (2.65 g, 17.7 mmol), and *p*-toluenesulfonic acid (*p*TSA) (30 mg, 0.16 mmol). The mixture was heated to 120 °C under nitrogen and stirred with a magnetic stirrer for 12 h. **Stage 2.** The system was then cooled to room temperature and connected to a vacuum distillation apparatus. After the vacuum reached 0.1 mmHg, the system was slowly heated to 200 °C in 2 h and then maintained at this temperature and pressure for 24 h. During this period, about 0.95 mL of colorless distillate was collected; in theory, 1.46 g or 1.3 mL of triethylene glycol should be collected. The magnetic stirring stopped toward the end of the polymerization due to the high viscosity of the system. The reaction product solidified quickly upon cooling and became a pale yellow solid at room temperature.

Purification. This material was dissolved in 30 mL of CH_2Cl_2 and precipitated in 300 mL of methanol. After the precipitate was filtered and dried, a pale yellow solid material was obtained (2.36 g, 94%): ^1H NMR δ 4.24 (t, J = 4.5 Hz, 4H), 3.70 (t, J = 4.5 Hz, 4H), 3.67 (s, 4H), 2.34 (t, J = 6.5 Hz, 4H), 1.62 (m, 4H), 1.32 (br s, 8H); ^{13}C NMR δ 173.4, 70.5, 69.2, 63.2, 34.0, 28.9, 24.7; IR (neat, cm^{-1}) 1128 (s), 1177 (s), 1249 (m), 1736 (vs), 2857 (s), 2929 (s).

2-[2-[*p*-[Tris(*p*-*tert*-butylphenyl)methyl]phenoxy]ethoxy]-ethanol (10). This compound was prepared as previously reported:[37] UV, $\epsilon = 2.88 \times 10^3$ at 266 nm (THF) with a baseline correction of 0.037 absorbance units from a Beer's law plot that gave absorbances between 0.1 and 0.9 for concentrations between 2×10^{-5} and 2×10^{-4} M.

Poly(butylene sebacate) (8b) (Sample SL-157). Stage 1. DMS (1.38 g, 6.0 mmol), 1,4-butanediol (1,4B) (1.19 g, 13.2 mmol), *p*TSA (18.3 mg, 0.096 mmol), and the mono[*p*-tris(*p*-*tert*-butylphenyl)methyl]-phenyl ether of di(ethylene glycol)] (**10**, 0.4286 g, 0.723 mmol) were mixed at 120 °C under nitrogen, 10 h; to give 0.6 mL of distillate.

Stage 2. The system was connected to a vacuum distillation apparatus and brought to 0.1 mmHg. The mixture was slowly heated to 200 °C in 2 h and then maintained at this temperature and pressure for 24 h. The magnetic stirring stopped toward the end of the polymerization due to the high viscosity of the system.

Purification. The white solid in methylene chloride (30 mL) precipitated in methanol (300 mL). A white powdery solid (1.72 g, 100%) was obtained after the precipitate was filtered and dried: T_m = 59.3 °C, no T_g (from DSC); ^1H NMR δ 7.10 (m, 0.44H), 6.78 (d, 0.04H), 4.09 (t, J = 5.5 Hz, 4H), 2.29 (t, J = 7.0 Hz, 4H), 1.70 (m, 4H), 1.61 (m, 4H), 1.30 (br s, 11.6 H); ^{13}C NMR δ 173.7, 130.6, 123.9, 110, 63.6, 34.2, 31.3, 29.0, 25.3, 24.8; IR ($CHCl_3$, cm^{-1}) 3021 (s), 2933 (m), 1727 (vs), 1223 (vs), 1177 (m); UV, A = 0.217 for a 1 cm cell, 1.78 mg in 10 mL of THF; calcd $\bar{M}_n$ = 5.7 kg/mol assuming 100% end-capping.

Poly(butylene sebacate) (8a) in the Presence of 18-Crown-6. Stage 1. MS (1.38 g, 6.0 mmol), 1,4B (1.19 g, 13.2 mmol), *p*TSA (18.3 mg, 0.096 mmol), and 18C6 (1.10 g, 4.2 mmol) were reacted at 120 °C under nitrogen for 10 h.

Stage 2. The system was connected to a vacuum distillation apparatus and brought to 0.1 mmHg. The mixture was heated to 200 °C in 2 h and then maintained at this temperature and pressure for 15 h.

Purification. The product in methylene chloride (30 mL) was precipitated in methanol (300 mL) two times to give a white powdery solid (1.55, g 90%): ^1H NMR same as above except there were no signals for end-blocking groups; no signals of 18-crown-6 or oligomeric glycols were found.

Purification of a Physical Mixture of Poly(triethyleneoxy sebacate) (7a) and 30-Crown-10 (1) (Sample 149, Table 2). A mixture of 1.30 g (4.11 mmol of repeat unit) of **7a** and 1.56 g (3.55 mmol) of **1** was dissolved in 3 mL of CH_2Cl_2 by stirring under N_2 at 70 °C. The solvent was allowed to evaporate, and the mixture was heated at 100 °C with stirring for 48 h. It was dissolved in 2 mL of CH_2Cl_2 and precipitated in 125 mL of methanol. The second precipitation was from 2 mL of CH_2Cl_2 into 75 mL of methanol. The polymer was then dissolved into 5 mL of CH_2Cl_2 and left in solution for 3 days before precipitation in 125 mL of methanol, to give 1.12 g (86%) of the polyester. The results are presented in entry 1, Table 2.

End-Blocked Poly[(triethyleneoxy sebacate)-rotaxa-(30-crown-10)] (11b) (Samples 2, 144, Table 2). Stage 1. DMS (1.80 g, 7.83 mmol), TEG (2.58 g, 17.2 mmol), 4,4-bis(*p*-*tert*-butylphenyl)-4-phenylbutanol (**9**, 130 mg, 0.31 mmol), 30C10 (3.80 g, 8.64 mmol), and *p*-TSA (24 mg, 0.13 mmol) were reacted at 120 °C under nitrogen for 10 h.

Stage 2. The system was connected to a vacuum distillation apparatus and brought to 0.7 mmHg. The mixture was heated to 260 °C in 2 h and then maintained at this temperature and pressure for 4 h.

Purification. The yellow viscous material was reprecipitated three times from 15 mL of CH_2Cl_2 in 300 mL of methanol. First precipitation: 0.84 g; ^1H NMR δ 7.25 (m, 0.96H), 4.24 (t, J = 45. Hz, 4H), 3.70 (t, J = 4.5 Hz, 4H), 3.67 (s, variable), 2.34 (t, J = 6.5 Hz, 4H), 1.62 (m, 4H), 1.32 (br s, 8H) (the resonance of 30-crown-10 occurs at δ 3.67); ^{13}C NMR δ 173.4, 70.5, 69.2, 63.2, 34.0, 28.9, 24.7 (the δ 70.5 peak corresponds to the carbon of 30-crown-10); IR (neat, cm^{-1}) 1127 (s), 1177 (m), 1736 (vs), 2859 (s), 2930 (s).

Hydrolysis of poly[(triethyleneoxy sebacate)-rotaxa-(30-crown-10)] (11b). A solution of poly[(triethyleneoxy sebacate)-rotaxa-(30-crown-10)] (0.50 g) and NaOH (0.20 g) in 20 mL of ethanol was heated at reflux and stirred under N_2 for 48 h. The resulting material was separated by preparative TLC and characterized by ^1H and ^{13}C NMR. 30-Crown-10 and tri(ethylene glycol) were isolated.

Poly[(triethyleneoxy sebacate)-rotaxa-(30-crown-10)] (11a) (Sample 230, Table 2). Stage 1. DMS (1.80 g, 7.83 mmol), TEG (2.58 g, 17.2 mmol), and *p*TSA (24 mg, 0.13 mmol) were reacted to 140 °C under nitrogen for 10 h.

Stage 2. 30C10 (3.80 g, 8.64 mmol) was added, and the system was brought to 0.3 mmHg, heated to 200 °C in 2 h, and then maintained at the temperature and pressure for 30 h.

Purification. The yellow viscous material was reprecipitated three times from 15 mL of CH_2Cl_2 in 300 mL of methanol: ^1H NMR δ 7.25 (m, 0.96 H), 4.24 (t, J = 4.5 Hz, 4H), 3.70 (t, J = 4.5 Hz, 4H), 3.67 (s, variable), 2.34 (t, J = 6.5 Hz, 4H), 1.62 (m, 4H), 1.32 (br s, 8H); ^{13}C NMR δ 173.4, 70.5, 69.2, 63.2, 34.0, 28.9, 24.7 (the signals at δ 3.67 and 70.5 are the resonances for 30-crown-10). Other spectral data are similar to those of polymer **11b**.

Poly[(triethyleneoxy sebacate)-rotaxa-(60-crown-20)] (12) (Sample 222, Table 2). Stage 1. DMS (1.80 g, 7.83 mmol), TEG (2.58 g, 17.2 mmol), and *p*TSA (24 mg, 0.13 mmol) were reacted at 140 °C under nitrogen for 48 h.

Stage 2. The system was cooled to 80 °C, 60C20 (3.80 g, 4.32 mmol) was added, and the system was brought to 0.1 mmHg and then heated to 175 °C in 2 h. The system was then heated over 16 h to 210 °C and maintained at this temperature and pressure for 20 h.

Purification. The yellow viscous material was reprecipitated three times from 10 mL of THF in 300 mL of H_2O. First precipitation, 0.84 g; second, 0.41 g; third, 0.20 g. Sepctral data of **12** were similar to those of **11**.

Poly[(triethyleneoxy sebacate)-rotaxa-(bis-*p*-phenylene-34-crown-10)] (13) (Sample 212, Table 2). Stage 1. DMS (2.00 g, 8.70 mmol), TEG (3.20 g, 21.3 mmol), and *p*TSA (20 mg, 0.12 mmol) were reacted at 140 °C under nitrogen for 4 h.

Stage 2. BPP (**4**, 1.34 g, 2.50 mmol) was added, and the system was brought to 0.1 mmHg. The system was heated to 210 °C over 2 h and then maintained at this temperature and pressure for 16 h.

Purification. The viscous product was reprecipitated three times from 10 mL of CH_2Cl_2 in 200 mL of CH_3OH: ^1H NMR δ 6.85 (s, variable) 4.24 (t, $J = 4.5$ Hz, 4H), 4.00 (m, variable), 3.80 (m, variable), 3.70 (m, variable), 2.34 (t, $J = 6.5$ Hz, 4H), 1.62 (m, 4H), 1.32 (br s, 8H) (the signals at δ 6.85, 4.00, 3.80, and 3.70 are due to BPP).

Poly[(butylene sebacate)-rotaxa-(30-crown-10)] (14) (Sample 234, Table 3). Stage 1. DMS (1.80 g, 7.83 mmol), 1,4B (1.55 g, 17.2 mmol), and *p*TSA acid (24 mg, 0.13 mmol) were reacted at 140 °C under nitrogen for 24 h.

Stage 2. 30C10 (3.80 g, 8.64 mmol) was added, and the system was brought to 0.1 mmHg. The system was heated to 180 °C over 2 h and then maintained at this temperature and pressure for 30 h.

Purification. The pale yellow viscous material in 15 mL of CH_2Cl_2 was precipitated in 300 mL of methanol several times: ^1H NMR δ 4.08 (t, $J = 5.5$ Hz, 4H), 3.67 (s, variable), 2.30 (t, $J = 7.0$ Hz, 4H), 1.71 (m, 4H), 1.62 (m, 4H), 1.30 (br s, 8H) (the peak at δ 3.67 is due to 30-crown-10); ^{13}C NMR δ 173.5, 70.5, 63.4, 34.2, 29.0, 25.3, 24.8 (the peak at δ 70.5 is due to 30-crown-10).

Poly[(butylene sebacate)-rotaxa-(42-crown-14)] (15) (sample SL-197, Table 3). Stage 1. DMS (0.3040 g, 1.321 mmol), 1,4B (0.2715 g, 3.013 mmol), *p*TSA (4.6 mg, 0.0242 mmol), and 42C14 (0.6404 g, 1.038 mmol) were reacted at 120 °C under nitrogen for 10 h.

Stage 2. The system was brought to 0.1 mmHg and heated to 180 °C over 2 h. The system was maintained at this temperature and pressure for 20 h.

Purification. The product in CH_2Cl_2 (10 mL) was precipitated in methanol (250 mL) three times: ^1H NMR δ 1.31 (br s, 8H), 1.61 (m, 4H), 1.71 (m, 4H), 2.29 (t, $J = 7.0$ Hz), 3.65 (s, variable, 42C14), 4.09 (t, $J = 5.5$ Hz); ^{13}C NMR δ 24.89, 25.30, 29.05, 34.23, 63.69, 70.53 (42C14), 173.77.

Poly[(butylene sebacate)-rotaxa-(60-crown-20)] (16) (Sample 240, Table 3). Stage 1. DMS (1.80 g, 7.83 mmol), 1,4B (1.55 g, 17.2 mmol), 60C20 (3.80 g, 4.32 mmol), and *p*TSA (24 mg, 0.13 mmol) were reacted at 140 °C under nitrogen for 5 h.

Stage 2. The system was brought to 0.1 mmHg and heated to 195 °C over 2 h. The system was maintained at this temperature and pressure for 20 h.

Purification. The viscous pale yellow material in 10 mL of THF was precipitated in 300 mL of H_2O. The spectral data of **16** were similar to those of **14**.

Poly[(butylene sebacate)-rotaxa-(bis-*p*-phenylene-34-crown-10)] (17a) (Sample 196, Table 3). Stage 1. DMS (0.83 g, 3.6 mmol), 1,4B (1.73 g, 19.2 mmol), and *p*TSA acid (15 mg, 0.087 mmol) were reacted at 125 °C under nitrogen for 12 h.

Stage 2. BPP (2.25 g, 4.20 mmol) was added, and the system was brought to 0.1 mmHg. The system was heated to 200 °C over 4 h and then maintained at this temperature and pressure for 20 h.

Purification. The viscous light brown material in 10 mL of THF was precipitated in 400 mL of methanol three times to yield a nearly colorless product: ^1H NMR δ 6.85 (s, variable), 4.08 (t, $J = 5.5$ Hz, 4H), 4.0 (m, variable), 3.80 (m, variable), 3.70 (m, variable), 2.30 (t, $J = 7.0$ Hz, 4H), 1.71 (m, 4H), 1.62 (m, 4H), 1.30 (br s, 8H) (the signals at δ 6.85, 4.0, 3.80, and 3.70 are due to BPP); ^{13}C NMR δ 173.5, 70.5, 63.4, 34.2, 29.0, 25.3, 24.8.

End-Blocked Poly[(butylene sebacate)-rotaxa-(bis-*p*-phenylene-34-crown-10)] (17b) (Sample 198, Table 3). Stage 1. DMS (0.55 g, 2.4 mmol), 1,4B (1.08 g, 12 mmol) 4,4-bis(*p*-*tert*-butylphenyl)-4-phenylbutanol (**9**, 70 mg, 0.16 mmol), and *p*TSA (10 mg, 0.058 mmol) were reacted at 150 °C under nitrogen for 4 h.

Stage 2. BPP (1.25 g, 2.33 mmol) was added, and the system was brought to 0.1 mmHg. The system was heated to 220 °C over 2 h and then maintained at this temperature and pressure for 24 h.

Purification. The product in 20 mL of CH_2Cl_2 was precipitated in 400 mL of methanol three times. The spectral data of **17b** were similar to those of **17a**.

Di[4,4-bis(*p*-*tert*-butylphenyl)-4-phenylbutyl] Sebacate (18). To a stirred solution of 0.20 mL (0.90 mmol) of sebacoyl chloride in di-(2-methoxyethyl) ether (6 mL) at 100 °C was added 74.2 mg (1.79 mmol) of 4,4-bis(*p*-*tert*-butylphenyl)-4-phenylbutanol (**9**), and the solution was stirred for 24 h. After solvent removal, the oily residue was purified by chromatography (silica gel/hexane) to give a 95% yield of crystalline product, mp 59.0−61.0 °C.

Diacetate of Poly(ethylene oxide), $\bar{M}_n$ 600. A solution of 3.0 g (10 mmol OH) of PEO 600, 12.0 g (153 mmol) of acetyl chloride, 7.0 g of pyridine, and 60 g of 1,2-dimethoxyethane was stirred at room temperature for 9 h. Removal of excess acid chloride, pyridine, and solvent in vacuo on a rotary evaporator produced pure product: ^1H NMR (Figure 11) δ 2.09 (s, 6H), 3.65 (m, 47H), 3.70 (t, $J = 5$ Hz, 4H), 4.22 (t, $J = 5$ Hz, 4H); ^{13}C NMR δ (Figure 11) 20.89, 63.52, 69.04, 70.48, 70.53, 170.96.

Acknowledgment. We gratefully acknowledge primary support of this research by the Polymers Program, Division of Materials Research, National Science Foundation, through individual investigator grants DMR-87-12428 and DMR-90-15729. Financial support from the NSF Science and Technology Center for High Performance Polymeric Adhesives and Composites at VPI&SU for a portion of this work is also much appreciated. Additionally, we thank our colleagues as follows: M. Siochi and the group of Prof. T. C. Ward for absolute GPC and DSC analyses; the group of Prof. J. E. McGrath for advice, discussion, and GPC analyses; and Prof. H. Marand and Dr. A. Prasad for helpful guidance, DSC experiments, and optical microscopy. We are grateful to Mukesh Bheda, Jean Sze, and Mark Gibson for synthesis of some of the macrocycles and to Sang-Hun Lee for the synthesis and NMR spectra of the diacetate of poly(ethylene glycol) 600.

JA942889N